LOWER BODY DYNAMICS FOR ROTATIONAL AND TRANSLATIONAL ACTIVITIES: CYCLING AND STAIR CLIMBING

A Thesis Submitted to
The Graduate School of İzmir Institute of Technology

In Partial Fulfillments of the Requirements for the Degree of

MASTER OF SCIENCE

in Mechanical Engineering

by
Bilal KARACAOĞLU

July 2023
İZMİR

We approve the thesis of **Bilal KARACAOĞLU**

Examining Committee Members:

Dr. Şenay Mihçin
Department of Mechanical Engineering,
Izmir Institute of Technology

Dr. Benay Uzer Yılmaz
Department of Mechanical Engineering,
Izmir Institute of Technology

Dr. Ebru Sayılgan
Department of Mechatronics
Engineering, Izmir University of
Economics

06/07/2023

Dr. Şenay Mihçin
Supervisor-Department of Mechanical
Engineering, Izmir Institute of
Technology

Prof. Dr. M. İ. Can Dede
Head of the Department of
Mechanical Engineering

Prof. Dr. Mehtap Eanes
Dean of the Graduate School

ACKNOWLEDGEMENTS

I would like to express my deepest gratitude to my supervisor, Dr. Şenay Mihçin, for her exceptional support, invaluable advice, and guidance throughout my thesis studies. Her expertise and dedication have been instrumental in shaping the success of this comprehensive project. I am truly fortunate to have had the opportunity to work under her mentorship, and I am grateful for the countless ways in which she has contributed to my personal and professional growth.

I am also grateful to Ahmet Mert Şahin and Mehmet Yılmaz, members of the Biomechanics and Motion Capture Systems Laboratory, for their unwavering support and assistance, regardless of the time or date. Their expertise and technical assistance have been invaluable in the execution and analysis of this research.

A special word of thanks goes to my sister, Hilal Karacaoğlu Sarigül, a physiotherapist, who played a critical role in this project by providing essential trainings and enlightening me about crucial aspects of the research area. Her insights and expertise have greatly enriched the quality of this study.

I would like to extend my heartfelt appreciation to my family for their unwavering belief in me and their continuous support throughout my academic journey. Their love, encouragement, and understanding have been a constant source of strength and motivation.

Lastly, I am indebted to my fiancé Burçe Akkurt who stood by my side during this thesis study, providing unwavering support, encouragement, and reminding me of the resilience within me.

Thank you all for your contributions and for being an integral part of this meaningful journey.

ABSTRACT

LOWER BODY DYNAMICS FOR ROTATIONAL AND TRANSLATIONAL ACTIVITIES: CYCLING AND STAIR CLIMBING

Evaluation of human movement performance in activities of daily living is an important component in clinical and rehabilitation settings. Motion capture technology is an effective method for objective evaluation of human motion. Here, movement kinematics and kinetic data are obtained from healthy individuals. In this thesis, it is detailed the daily life movements based on stair climbing and cycling. The aim of this study is to examine the effects of human movement on the kinetic and kinematic variables of the hip joint during stair climbing and descending. Data were collected using the Qualisys motion capture system, force plates, ladder and bicycle. By analyzing data from different individuals here, great potential information can be gained for predicting the recovery and progression of movement for patients. In the future, the development of personalized therapy protocols in rehabilitation with individualized progression can be offered. Optimum design parameters for the individual device and exercise device can be obtained, and if the relevant joints are supported with implants, it is possible to obtain the necessary boundary conditions for personalized implant design and to collect the necessary data for implant design. The Results and Discussion Chapter illustrates and tabulates the calculated results.

In the Findings and Discussion section of the thesis, the calculated results of the study are included. This section provides a comprehensive analysis of the data collected, highlighting the observed patterns, trends, and variations in hip joint kinematics and kinetics during selected activities. The Discussion section delves into the significance of the findings by comparing the findings with the available literature, identifying similarities and differences, and offering possible explanations for observed variations.

ÖZET

DÖNME VE ÖTELEME AKTİVELERİ İÇİN ALT VÜCUT DİNAMİKLERİ: BİSİKLET BİNME VE MERDİVEN ÇIKMA

Günlük yaşam aktivitelerinde insan hareket performansının değerlendirilmesi, klinik ve rehabilitasyon ortamlarında önemli bir bileşendir. Hareket yakalama teknolojisi, insan hareketinin objektif olarak değerlendirilmesi için etkili bir yöntemdir. Burada hareket kinematiği ve kinetik veriler sağlıklı bireylerden elde edilir. Bu tezde, merdiven çıkma ve bisiklete binmeye dayalı günlük yaşam hareketlerini detaylandırılmaktadır. Bu çalışmanın amacı, merdiven çıkma ve bisilet sürme sırasında insan hareketinin kalça ekleminin kinetik ve kinematik değişkenleri üzerindeki etkilerini incelemektir. Veriler, Qualisys hareket yakalama sistemi, kuvvet plakaları, merdiven ve bisiklet kullanılarak toplanmıştır. Burada farklı bireylerden alınan verileri analiz ederek, hastalar için hareketin iyileşmesini ve ilerlemesini tahmin etmek için büyük potansiyel bilgiler elde edilebilir. Gelecekte, bireyselleştirilmiş ilerleme ile rehabilitasyonda kişiselleştirilmiş terapi protokollerinin geliştirilmesi önerilebilir. Bireysel cihaz ve egzersiz cihazı için optimum tasarım parametreleri elde edilebilir ve ilgili eklemler implantlarla desteklenirse, kişiye özel implant tasarımı için gerekli sınır koşullarının elde edilmesi ve implant tasarımı için gerekli verilerin toplanması mümkündür. Sonuçlar ve Tartışma Bölümü, hesaplanan sonuçları gösterir ve tablo haline getirir.

Tezin sonuçlar ve tartışma bölümünde ise çalışmanın hesaplanan sonuçlarına yer verilmiştir. Bu bölüm, seçilen aktiviteler sırasında kalça eklemi kinematiği ve kinetiğinde gözlemlenen modelleri, eğilimleri ve varyasyonları vurgulayarak toplanan verilerin kapsamlı bir analizini sunar. Tartışma bölümü, bulguları mevcut literatürle karşılaştırarak, benzerlikleri ve farklılıkları belirleyerek ve gözlemlenen varyasyonlar için olası açıklamalar sunarak bulguların önemini araştırır.

ABBREVIATIONS

ADLs: Activities of Daily Life

CAST: Calibrated Anatomical System TechniqueEMG:

Electromyography

EMS: Electromagnetic Systems

IMUs: Inertial Measurement Units

ISB: International Society of Biomechanics

MOCAP: Motion Capture Systems

MRI: Magnetic Resonance Imaging

OMCs: Optical Motion Capture Systems

QTM: Qualisys Track Manager

ROM: Range of Motion

THA: Total Hip Arthroplasty

P.C.F: Participant Consent Forms

P.I.S: Participant Information Sheet

TABLE OF CONTENTS

LIST OF FIGURES

Figure **Page**

LIST OF TABLES

CHAPTER 1

INTRODUCTION

Biomechanics of daily life movements examines how the human body moves during daily activities and the physical effects of these movements. The human body uses interactions between muscles, bones, joints and other tissues to perform many different movements. Biomechanics helps us understand how movement can be optimized by analyzing these interactions and the ways the body moves. The kinetic and kinematic impact of biomechanics can be used to understand and optimize daily life movements. The use of this information is important, especially in the fields of sports, exercise and rehabilitation. Understanding how movements occur, how muscles work, and at what angles joints move can be helpful to improve movement performance and reduce the risk of injury. This information can be used in many areas such as improving sports performance, optimizing rehabilitation processes, developing ergonomic designs and reducing the risk of injury.

Cycling and stair activities involve different biomechanical movements that affect various parts of the body. Cycling and stair activities both involve the use of the lower body and require the application of certain biomechanical principles to perform them efficiently and safely. When cycling, biomechanics involves the transfer of energy from the legs to the pedals that propels the bike forward. The pedal stroke consists of four phases: downstroke, upstroke, backstroke, and recovery. During a descent, the quadriceps muscles contract to extend the leg, while the calf muscles contract to plantar flex the foot. The upstroke involves contracting the hamstring muscles to flex the leg, while the hip flexors and shin muscles contract to dorsiflex the foot. The supine involves activating the hip muscles and hip extensors to move the knee forward while lengthening the hamstrings and calf muscles. Finally, during the recovery phase, the leg is raised and reset for the next pedal stroke.

The stair-climbing biomechanics movement cycle involves repeated phases as you climb stairs. These stages require effective functioning of the muscle structure. Leg muscles play an important role when climbing stairs. The front thigh muscles, called the quadriceps femoris, are activated when stepping on a ladder and trying to push body

weight up. These muscles create force on the knee joint, allowing the body to move upwards. At the same time, the calf muscles (gastrocnemius and soleus muscles) play an important role when climbing stairs. These muscles help push the body upward by applying force to the ankle joint.

Other muscle groups are also activated in the process of climbing stairs. The gluteus muscles, called the gluteus maximus, generate force to push the body up. Hip flexors (iliopsoas muscles) and hip abductors (gluteus medius and minimus muscles) work to provide balance and stability. Shoulder and arm muscles are also used during stair climbing. In particular, muscles such as the biceps brachii (forearm muscle) and deltoid (shoulder muscle) function to hold stairs and stabilize the body. The stair climbing biomechanics movement cycle involves the interaction and synergy of these muscle groups. Body position and muscle activation ensure that the stair climbing movement is performed in an efficient and balanced manner.

1.1. Hip Anatomy

The hip joint is known as a large joint located where the femur (thigh bone) and pelvis (pelvis bone) as shown in figure 1 meet. It is one of the largest and strongest joints in the body. The hip joint is important for mobility and providing support.

The hip joint is formed between the ball-shaped head of the femur and the socket of the pelvis called the acetabulum. The joint is supported by bony structures as well as ligaments, muscles and a connective tissue bag called a capsule. Ligaments play an important role in stabilizing the joint and preventing its excessive movement.

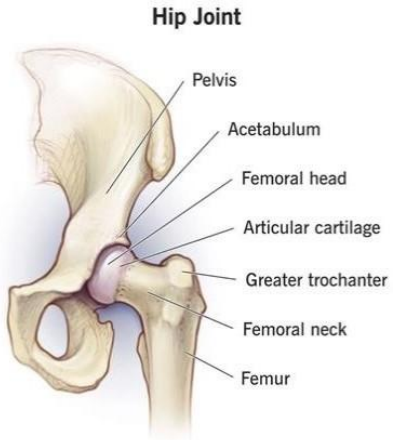

Figure 1. Hip Joint

The hip joint has multi-directional mobility. It can make forward-backward, sideways opening, inward turning and outward turning movements in a straight line. These movements are important in daily activities such as walking, running, climbing stairs. The hip joint is a joint that bears most of the body weight. Therefore, various problems may occur as a result of overloading or traumas in the joint.

The hip joint enables movement in three different directions known as flexion-extension, abduction-adduction, and internal-external rotation. These movements take place in three specific planes: sagittal plane, frontal (coronal) plane, and transverse plane. Figure 2 provides a visual representation of the rotations and planes involved in hip joint movement. The hip joint permits flexion-extension, abduction-adduction, and internal-external rotation, each occurring in the sagittal, frontal, and transverse planes, respectively.

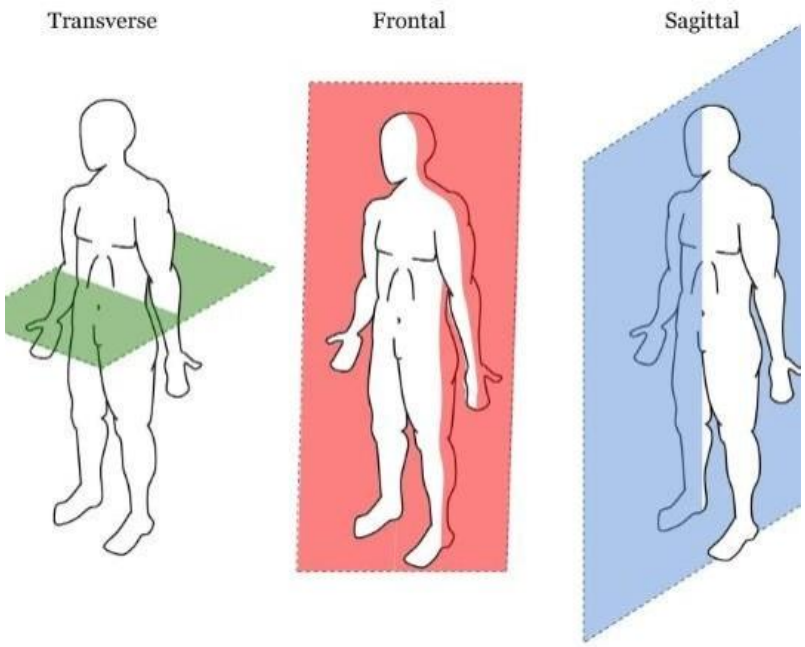

Figure 2. Three Different Directions

1.1.1. Sagittal Plane Movement

Sagittal plane movement refers to the forward-backward motion that occurs in the body along an imaginary plane that divides it into left and right halves. In the context of the hip joint, sagittal plane movements primarily involve flexion and extension.

- Flexion: Hip flexion refers to the movement of bringing the thigh bone (femur) forward, towards the front of the body. This movement decreases the angle between the thigh and the torso. For example, when you lift your leg to take a step, your hip joint undergoes flexion.
- Extension: Hip extension is the opposite movement of flexion. It involves moving the thigh bone backward, away from the front of the body, thus increasing the angle between the thigh and the torso. Examples of hip extension include pushing your leg backward while walking or standing up from a seated position.

These flexion and extension movements in the sagittal plane are crucial for activities like walking, running, climbing stairs, and performing various lower body exercises. The muscles involved in these movements include the hip flexors (e.g., iliopsoas) for flexion and the hip extensors (e.g., gluteus maximus, hamstrings) for extension.

It's important to note that while sagittal plane movements predominantly involve flexion and extension, the hip joint also allows some degree of abduction-adduction and internal-external rotation, as mentioned earlier, in different planes of movement.

1.1.2. Frontal plane movements

Frontal plane movements, also known as coronal plane movements, occur along an imaginary plane that divides the body into front and back halves. In the context of the hip joint, frontal plane movements primarily involve abduction and adduction.

- Abduction: Hip abduction refers to the movement of the thigh bone (femur) away from the midline of the body, towards the side. This movement increases the space between the thighs. For example, when you spread your legs apart to the sides, your hip joints undergo abduction.
- Adduction: Hip adduction is the opposite movement of abduction. It involves bringing the thigh bone back towards the midline of the body, closing the space between the thighs. For instance, when you bring your legs together after spreading them apart, your hip joints undergo adduction.

These abduction and adduction movements in the frontal plane play important roles in activities such as side-stepping, lateral leg raises, and maintaining stability during movements that involve shifting weight from one leg to another. The muscles involved in these movements include the hip abductors (e.g., gluteus medius, tensor fasciae latae)

for abduction and the hip adductors (e.g., adductor longus, adductor magnus) for adduction. While sagittal and frontal plane movements are the primary motions of the hip joint, the joint also allows internal-external rotation as mentioned earlier, completing the three degrees of freedom and providing a wide range of movement possibilities for the hip.

1.1.3. Transverse plane movements

Transverse plane movements occur along an imaginary plane that divides the body into upper and lower halves. In the context of the hip joint, transverse plane movements primarily involve internal and external rotation.

- Internal Rotation: Hip internal rotation refers to the inward rotation of the thigh bone (femur) towards the midline of the body. This movement involves the rotation of the thigh bone within the hip socket, with the knee turning towards the midline. For example, when you cross one leg over the other while seated, your hip joint undergoes internal rotation.
- External Rotation: Hip external rotation is the opposite movement of internal rotation. It involves the outward rotation of the thigh bone away from the midline of the body. In this movement, the thigh bone rotates within the hip socket, and the knee turns away from the midline. For instance, when you spread your legs apart and rotate your toes outward, your hip joints undergo external rotation.

Transverse plane movements at the hip joint are important for activities like pivoting, turning, and rotating the lower body. They contribute to actions such as swinging the leg during walking or performing exercises that involve twisting movements. The muscles involved in these movements include the hip external rotators (e.g., piriformis, gemellus muscles) for external rotation and the hip internal rotators (e.g., gluteus medius, tensor fasciae latae) for internal rotation. By combining movements in the sagittal, frontal, and transverse planes, the hip joint enables a wide range of motion, allowing for activities such as walking, running, squatting, and various athletic. Cycling and stair climbing activities involve a series of biomechanical movements that affect the muscles and joints in the hip area. Here are some key points about the biomechanics of the hip in these activities:

Ride a bike:

- Hip Flexion: While cycling, they constantly flex your hips. While sitting on the

bike, you must flex your hips to apply power to the bike's pedal.

- Hip Extension: When you apply force by pressing the pedals, your hips should extend. This move is important for increasing the speed of the bike and pushing your body weight up.
- External Rotation: When cycling, your hips rotate outward. This movement is important to prevent your knees from moving inwards as you apply power to the bike's pedal.

Stair Climbing:

- Hip Flexion: While climbing stairs, you must flex your hips with each step. This move allows you to step on the ladder by raising your leg up.
- Hip Extension: When climbing steps, you need to extend your hips. This move helps push your body weight upwards.
- External Rotation: As you climb stairs, your hips rotate outward with each step. This is important to prevent your knees from moving inwards and to provide stability.

Both activities work your hip muscles, specifically the hip flexors (front thigh muscles), hip extensors (gluteus muscles), and hip external rotators (gluteus medius). These muscles create force on the hip joint, making cycling and stair climbing possible.

However, there may be individual differences in cycling and stair climbing activities. Biomechanical movements may vary depending on factors such as the individual's anatomy, condition and technical skills. If you are planning a prolonged or intense activity, working with a sports physiotherapist or trainer is important to learn the right techniques and prevent potential injury.

The sagittal plane is the primary focus in studies on bicycle movement, as it involves the major movement and power generation during cycling. In the sagittal plane, the hip and knee joints exhibit the largest ranges of motion. Hull M. Hawkins DA.(1990) İnvestigated on bicycle movement. The knee is bent at approximately 75 degrees, ranging from 110 degrees at top dead center (TDC) to 25-35 degrees at bottom dead center (BDC) during the pedal stroke,. The hip joint shows approximately 55 degrees of sagittal plane movement, while the ankle joint moves approximately 25 degrees during cycling.

David J.S. Wadsworth(2019) is indicate that It is important to note that the absolute hip angle is not commonly reported in the literature due to measurement difficulties arising from the forward-sloping body position of cyclists and variations in

the anatomical landmarks used in different studies. However, it is crucial to highlight that there is a significant peak in hip flexion at the top dead center (TDC) of the pedal stroke, which may cause discomfort in individuals with symptomatic hip joint disorders. During the power phase or push-up phase of cycling, both the hip and knee joints extend in the sagittal plane, while ankle movement is more variable. Typically, the ankle dorsiflexes during the first half of the power phase and plantar-flexes at the end of the powerful push-down. Hull M. Hawkins DA.(1990) were conducted that the force applied to the crank that propels the bike forward typically occurs between 10 degrees and 170 degrees, peaking at the 90-degree position when the crank arm is horizontal. The propulsive forces are usually not generated during the push-up phase, which is characterized by minimal electromyographic (EMG) activity in the major leg muscles. The propulsion force is created when the contralateral leg is in its propulsion phase, while the ipsilateral leg is in a relatively relaxed state during the push-up phase. The quadriceps, gluteus maximus, hamstrings, and gastrocnemius muscles primarily contribute to the propulsive force.

Stair climbing activities also involve a complex biomechanical movement that requires the activation of multiple muscle groups. When climbing stairs, the quadriceps muscles are activated to extend the knee, while the hip muscles and hamstring muscles contract to extend the hip joint. The calf muscles contract to plantar flex the foot, assisting in pushing off the step. During descent, the quadriceps muscles act as shock absorbers to control the descent speed, while the calf muscles contract eccentrically to control the movement of the foot and lower leg.

Andriacchi et al. (1980) conducted a study on ten young healthy male subjects to analyze hip, knee, and ankle joint angles and moments during stair climbing. Their findings indicated that the sagittal plane exhibited the greatest range of motion (ROM). Specifically, during stair climbing, the hip joint required approximately 15 to 20 degrees more ROM compared to level walking. During stair descent, hip angles ranged from 20 to 30 degrees at the beginning of the stance phase and gradually flexed to 10 to 15 degrees at the end of the stance phase.

The study conducted by Riener et al. (2002) aimed to explore the biomechanics and motor coordination involved in stair climbing at various inclinations. The researchers observed that as the angle of inclination of the staircase increased, there were corresponding increases in joint ranges and maximum flexion angles. Specifically, during stair ascent, the maximum flexion angle of the hip joint was found to be 12.4% greater at maximum inclination compared to the minimum inclination. This finding highlights the

significant impact of the angle of inclination on the kinematics of stair climbing.

The results of this study emphasize that the inclination of the staircase plays a crucial role in determining the joint movements and ranges during stair climbing. Understanding the effects of incline on the biomechanics of stair climbing can inform rehabilitation programs, architectural design considerations, and the development of assistive devices to optimize safety and efficiency in stair negotiation.

In a study conducted by Nadeau et al. (2003), a comparison was made between stair climbing and level walking in healthy adults aged over 40 years. The researchers focused on analyzing the differences in movement patterns in the frontal and sagittal planes.

Regarding the frontal plane movement profiles, the study found that the main variations occurred at the hip joint. During both stair climbing and level walking, the peak hip abduction was observed to be less than 5 degrees and typically occurred just after toe-off.

In the sagittal plane, the differences in kinematic profiles were more prominent at the knee and ankle joints compared to the hip joint. While the hip profiles were similar between level walking and stair climbing, it was noted that a more flexed hip position was consistently observed throughout the gait cycle during stair climbing. It is important to acknowledge that the range of motion (ROM) differences between level walking and stair climbing can be influenced by various factors, including the characteristics of the staircase and individual characteristics. Compensatory mechanisms were found to primarily occur at the knee joint, with secondary compensations occurring at the ankle and hip joints, as highlighted in the study by Riener et al. (2002). These findings contribute to our understanding of the biomechanical differences between stair climbing and level walking, particularly in relation to hip joint motion and the compensatory mechanisms employed by individuals. Such knowledge can inform rehabilitation strategies and the design of interventions targeted at improving stair climbing abilities and addressing gait abnormalities in older adults.

Several studies have examined the hip moment patterns during stair ascent and descent, revealing variability in their findings. Andriacchi et al. (1980) and Costigan et al. (2002) observed external flexor moments during stair ascent. Costigan et al. specifically reported an external hip flexion moment of 0.8 Nm/kg (SD 0.12). On the other hand, McFadyen and Winter (1988) and Riener et al. (2002) reported internal hip extensor moments during stair ascent but noted internal hip flexor moments at the end of

the stance phase.

In contrast, Salsich et al. (2001) reported a brief period of internal hip flexor moment at the beginning of the stance phase, followed by an internal hip extensor moment during stair ascent. It is important to consider that the position of the trunk can influence the line of the ground reaction force relative to the hip joint, thereby affecting the hip joint moments observed during stair climbing. These differing findings suggest that hip moment patterns during stair ascent and descent can vary depending on the specific study and measurement techniques employed. The complex interplay between muscle activation, joint angles, and body mechanics likely contributes to these variations in hip moment patterns. Further research is needed to better understand the underlying mechanisms and functional implications of these hip moment patterns during stair climbing. Both cycling and stair climbing require balancing the body, utilizing muscle strength, and coordinating joints at the correct angles. By understanding the biomechanical principles involved, individuals can develop more efficient and safe techniques for cycling and stair climbing.

In this thesis, he details the daily life movements based on stair climbing and cycling. The aim of this study is to examine the effects of human movement on hip joint kinematics and kinetic variables during stair climbing and cycling. Data will be collected using the Qualisys motion capture system, force plates, ladder and bike. By analyzing data from different individuals here, great potential information can be gained for predicting the recovery and progression of movement for patients. In the future, the development of personalized therapy protocols in rehabilitation with individualized progression can be offered. Optimum design parameters for the individual device and exercise device can be obtained, and if the relevant joints are supported with implants, it is possible to obtain the necessary boundary conditions for personalized implant design and to collect the necessary data for implant design.

CHAPTER 2

METHODOLOGY

This section provides a comprehensive explanation of the chapter, including the procedure, experimental protocol for data collection, materials utilized in the experiment, and the methodology employed for conducting the analysis.

2.1. Procedure

In this section, the study's procedure is elucidated, covering essential aspects such as obtaining Ethics Committee Approval, describing the consent process, and outlining the criteria for participant selection.

2.1.1. Ethics Committee Approval and Consent

Obtaining ethical permission is a mandatory requirement when collecting data from human subjects, especially when involving healthy volunteers, as stipulated by the law. In compliance with this requirement, the study received ethical permission from the ethical committee of the Medical Faculty of İzmir Katip Çelebi University. Once the ethics permission was granted, Participant Information Sheets (P.I.S) and Participant Consent Forms (P.C.F) were prepared to ensure that volunteers were adequately informed. The P.I.S provided participants with detailed information about the study's procedure, data collection methods, handling of classified information, exclusion criteria, potential benefits, and the rights they held as participants during the study.

2.1.2. Participation Criteria

To ensure the collection of reliable data, the study emphasizes the importance of recruiting healthy volunteers who meet specific participation criteria as shown in table1. These criteria are divided into two categories: inclusion criteria and exclusion criteria, which are aimed at forming a robust and trustworthy database.

Table 1. Participation Criteria

Inclusion Criteria	Exclusion Criteria
• Participant must be 18 years old or older than 18 years old. • No suspicion or diagnosis of Covid-19 during the experiment. • The HES code must be received.	• History of trauma in the lower body (hip, knee, foot, ankle). • Implants in the lower body (hip, knee, foot, ankle). • Pregnancy in female volunteers. • Allergies related to the materials to be used in the experiment. • Body Mass Index (BMI) of 30 or above.

2.2. Selected Activities of Daily Life

A selection was made to perform two activities in the daily life with the participation of volunteers. These selected activities were recorded using the Qualisys (Gothenburg, Sweden) optical motion capture system.

Table 2. Determined Daily Life Activities

No.	Activity
1	Stair Climbing
2	Cycling

2.2.1. Protocol

The Protocol section provides detailed explanations of each identified daily life movement and its impact on the hip joint. It also outlines how these selected movements will be executed by the volunteers. The experiments are conducted in accordance with the established protocol.

2.2.1.1. Stair Climbing

During stair ascent and descent, the movement of the lower limbs follows cyclical pattern similar to level walking. The gait cycle for both tasks can be divided into two phases: the stance (support) phase and the swing phase. The distribution of time spent in

the swing and stance phases differs between stair ascent (66% stance: 34% swing) and stair descent (60% stance: 40% swing).

In the context of stair climbing, the stance and swing phases are further divided into specific sub-phases. The stance phase during stair ascent consists of three sub-phases as shown in figure 3:

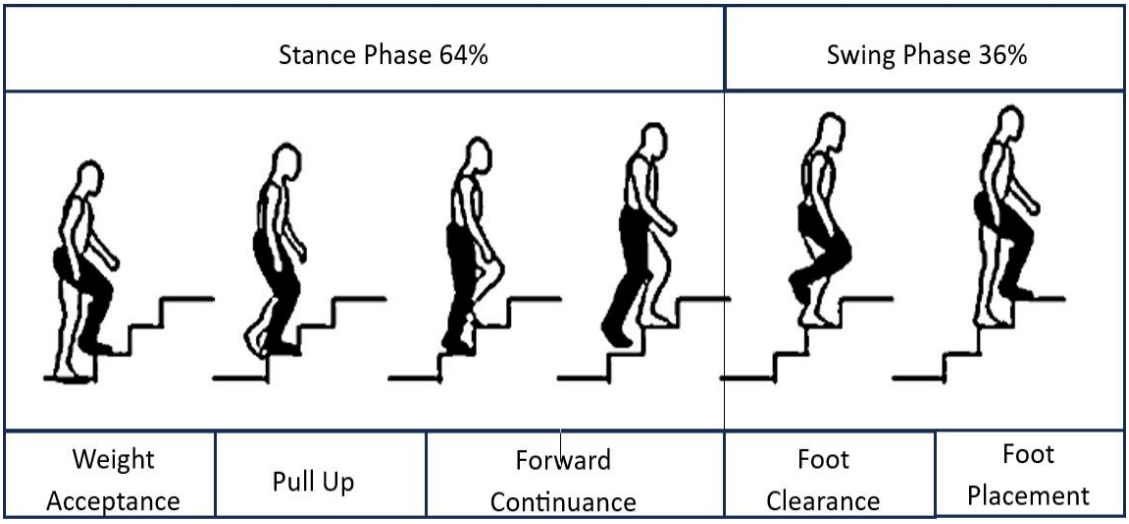

Figure 3. Stair Climbing Gait Cycle

- Weight Acceptance (WA): This sub-phase involves the initial movement of the body to position it optimally for being pulled up to the next step. It occurs when the foot makes contact with the stair, and the body weight is transferred from the previous step to the current one.
- Pull Up (PU): The main progression of ascending from one step to the subsequent step takes place in this sub-phase. The leg muscles work to lift the body upward, generating the necessary force to overcome gravity and move to the next step.
- Forward Continuance (FC): Once the complete ascent of a step has occurred, the forward progression continues. The body keeps moving forward onto the next step, ensuring a smooth transition between steps.

On the other hand, the swing phase during stair ascent can be divided into two sub-phases:

- Foot Clearance (FCL): This sub-phase involves bringing the leg up and over to the next step while ensuring that the foot remains clear of the intermediate step. It allows for a smooth leg movement during stair climbing.

- Foot Placement (FP): In this sub-phase, the swing leg is lifted, and the leg is positioned for foot placement on the next step. It involves preparing the leg for a secure and stable landing on the step.

During stair climbing activity, hip abduction (legs out sideways), hip internal and external rotation, and hip joint angle play an important role.

- Hip Abduction: Hip abduction is the movement of spreading the legs to the sides while climbing stairs. This movement activates the hip muscles (especially the gluteus medius). The gluteus medius muscle controls the lateral extension of the legs, keeping the hip stable. When climbing stairs, hip abduction is important so that the legs are placed on the stair step with each step. This movement provides balance and allows the legs to move stably.
- Hip Internal Rotation and External Rotation: Hip internal rotation means inward rotation of the leg, while external rotation of the hip means outward rotation of the leg. During stair climbing, these rotational movements occur as the legs are placed on the stair step. Hip internal rotation and external rotation help to properly position the legs and stabilize the stair climbing motion.

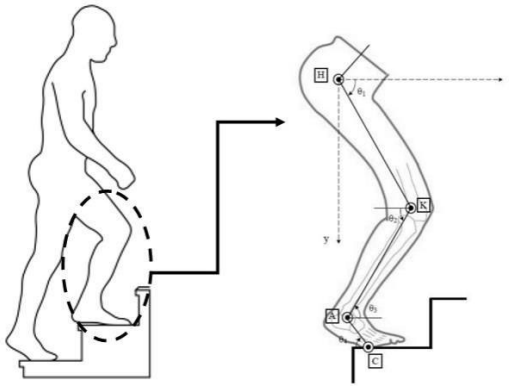

Figure 4. Hip Joint Angle Free Body Diagram

- Hip Joint Angle: Hip joint angle refers to the degree of bending or extension of the hip joint. During stair climbing, hip joint angle may need to change to properly position the legs on the stair step. The hip joint usually does more flexion (twisting) movements so that the legs can gain enough height to climb the stair step. The hip joint angle allows the legs to move upward and perform the stair climbing activity.

- Hip Moment: The hip moment is the rotational force that occurs in the hip joint while climbing stairs. This moment provides stability of the hip joint and controls the movement of the legs. Hip moment is essential for maintaining balance and control of body weight and movement during stair climbing. This moment is created by the coordinated work of the hip muscles (gluteus muscles, hamstrings, etc.). The hip moment supports a balanced movement that is necessary for placing the legs on the stair step, raising and advancing the body.
- Joint Reaction Force: Joint reaction force is the force on the hip joint during stair climbing. This force occurs to balance the effect of body weight and movement on the stair step. Joint reaction force tests the endurance of the hip joint during stair climbing and dissipates the stress that occurs when the hip joint is loaded. This force provides proper loading to the hip joint and protects the joint. In addition, the joint reaction force supports the stability of the movement by ensuring that the leg muscles and other stabilizer muscle groups work correctly.

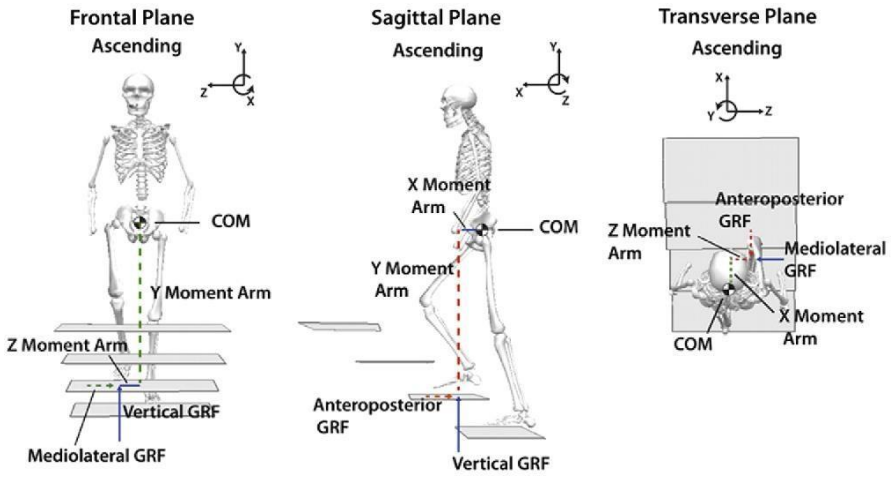

Figure 5. Diagram of external moment arms and ground reaction forces (GRF) in three anatomical planes while climbing stairs.

The harmonious execution of these movements ensures stability when climbing stairs, supports the correct positioning of the legs and ensures safe movement. However, hip biomechanics can differ between individuals. A person's posture, muscle strength, flexibility, and other factors can affect how these movements are performed. A qualified physiotherapist or specialist can evaluate to recommend the right techniques and exercises to suit individual needs.

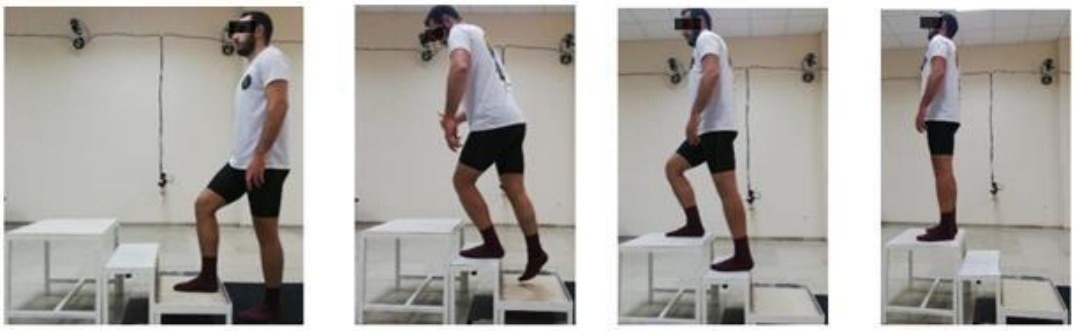

Figure 6. Stair Climbing

The stance phase refers to the duration when the foot is in contact with the ground during the gait cycle and it is illustrated in Figure 3.It starts with the initial contact of the foot and concludes when the foot lifts off the ground, also known as toe-off. On the other hand, the swing phase encompasses the entire duration of the foot being in the air. It commences after toe-off and terminates with the subsequent initial contact of the foot.

The practice of stair climbing involves a ladder with three steps, as depicted in Figure 6. On the first step of the ladder, there is a force platform in place. To gather reliable data from both legs, two distinct movements are performed: stair climbing and stair descending. These movements require different foot placements, with the left foot leading during one movement and the right foot leading during the other. For accurate data analysis, it is crucial to ensure that the ascending movement begins with either the right or left foot and that the descending movement concludes with the opposite foot (left or right) as shown in figure 6. This consistent pattern enables consistent data comparison between the two legs.

2.2.1.2. Cycling

The hip angle of a cyclist's pedal stroke refers to the position of the hip joint during the cycling motion. It can vary depending on factors such as bike fit, riding style, and individual biomechanics. During the downstroke phase of the pedal stroke, when the leg is extending and applying force to the pedal, the hip angle typically opens up, meaning the hip joint moves towards extension. This allows the cyclist to generate power and push down on the pedal. On the upstroke phase, when the leg is flexing and returning to the top of the pedal stroke, the hip angle tends to close or flex. This helps in maintaining a

smooth and efficient pedal motion and allows for better engagement of the muscles involved.

It's important to note that the optimal hip angle can vary among individuals, and bike fit adjustments, such as saddle height and fore/aft position, can influence the hip angle during the pedal stroke. Working with a professional bike fitter or sports scientist can help cyclists find their optimal hip angle for efficient and comfortable riding.

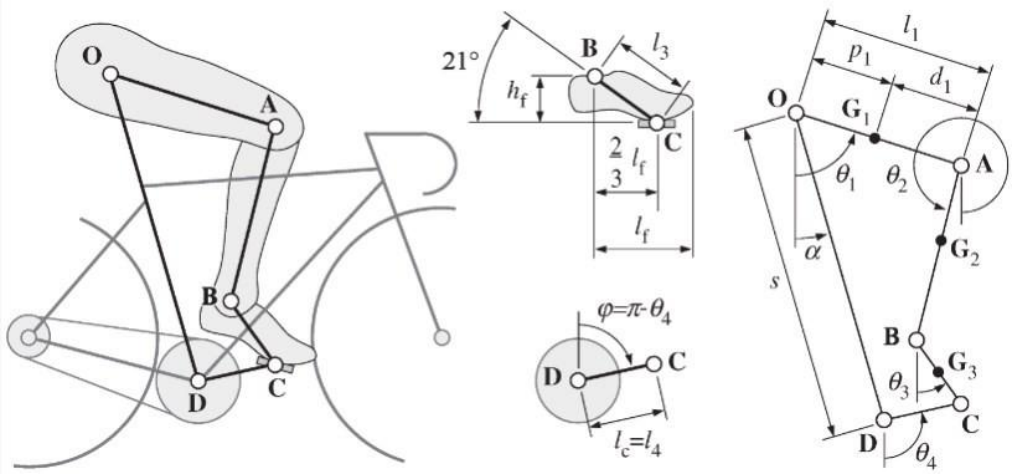

Figure 7. Free Body Diagram of Cycling

The freely moving body diagram of the bicycle-foot system, characterized based on anthropometric scale factors, is shown in Figure 7. It represents the adopted skeletal model and provides the basic terminology used to describe the system's kinematics. The vector $\theta = [\theta 1\ \theta 2\ \theta 3\ \theta 4]$ assumes a positive rotation in the counterclockwise direction, and it encompasses the absolute orientation with respect to the vertical axis of the system's four movable segments. The subscript i (i = 1:4) refers respectively to the symbols representing the thigh, leg, foot, and crank. The length of the i-th link is denoted by l^{i}.

The OD constant distance s (1) is determined by the following formula:

$$s = 1.09hins - lc = 1.09(0.48h) - lc \quad (1)$$

To solve the position problem using a closed loop along the path $O-^{T}-B-C-D-O$, we can define the position of each point (2) along the path as variables and set up a system of equations based on the geometric relationships between these points. Let's denote the coordinates of each point as follows:

$$\begin{matrix} (\quad,\quad) \\ (\quad,\quad) \\ (\quad,\quad) \\ (\quad,\quad) \\ (\quad,\quad) \end{matrix} \tag{2}$$

We can establish the following system of equations based on the closed loop:

$$\sum_{i=1}^{3} l_i \sin\theta_i - l_4 \sin\theta_4 - s\sin\alpha = 0 \tag{3}$$

$$\sum_{i=1}^{3} l_i \cos\theta_i - l_4 \cos\theta_4 - s\cos\alpha = 0 \tag{4}$$

Given that all the length variables in Equation (3,4) are known, and as shown in Figure 7, the crank angle increases clockwise from the top dead center (TDC), we can relate 4 to by the following relation:

$$\theta_4(\varphi) = \pi - \varphi \tag{5}$$

In this relation, $\theta 4$ is showed with equation, 5 represents the angle between the crank and the connecting rod, and φ is the crank angle. Since φ increases clockwise from the top dead center (TDC), the relation above accounts for this clockwise rotation. This relation can be used to determine the value of $\theta 4$ at any given crank angle φ, given the known value of α and the geometric configuration of the crank-connecting rod mechanism. With this information, the system of equations can be fully defined and solved to obtain the positions of points A, B, C, and D along the path $O-A-B-C-D-O$ for different crank angles during the motion.

To establish a relation between the foot angle 3(6) and the crank angle , got from QTM data was used. The data has been fitted using a law of the following form:

$$3 = 3(\ ) \tag{6}$$

For this purpose, calculations are made by using the data obtained from the experiment.

$$\theta_3(\varphi)=\gamma_a+\gamma_b\sin(\varphi-\text{[illegible]}) \quad (7)$$

To find the two remaining unknowns, 1 and 2, as functions of , we need to solve the system of equations (3,4) in combination with Equations (5) and (7), once the relations 3( ) and 4( ) are defined from the experimental data. The system of equations (3,4) relates the positions of points A, B, C, and D with respect to the starting point O, while Equations (5) and (7) define the geometric relationships between the different angles involved in the mechanism. Once we have the positions of points A, B, C, and D as functions of using the relations 3( ) and 4( ), we can find the angles 1 and 2 by considering the geometry of the mechanism.

The linear form for the velocity problem can be obtained by taking the derivative of the position equations(8,9) with respect to time. This yields the equations that relate the angular velocities of the different links in the mechanism.

$$J_1[\theta_1\ \theta_2]^T + J_2[\theta_3\theta_4]^T = 0 \quad (8)$$

$$[\theta_1\ \theta_2]^T = -J_1^{-1}J_2[\theta_3\ \theta_4]^T \quad (9)$$

For the system of equations you mentioned earlier, the Jacobian matrices(10,11) can be defined as follows:

$$J_1 = \begin{bmatrix} l_1\sin\theta_1 & l_2\sin\theta_2 \\ l_1\cos\theta_1 & l_2\cos\theta_1 \end{bmatrix} \quad (10)$$

$$J_2 = \begin{bmatrix} l_3\sin\theta_3 & -l_4\sin\theta_4 \\ l_3\cos\theta_3 & -l_4\cos\theta_4 \end{bmatrix} \quad (11)$$

To obtain the expressions for accelerations, we need to take the second derivative of the position equations(12).

$$[\theta_1\ \theta_2]^T = J_1^{-1}\left(J_2[\theta_3\ \theta_4]^T + [\theta_1^2\ \theta_2^2\ \theta_3^2\ \theta_4^2]^T\right) \quad (12)$$

where the Jacobian related to the centrifugal terms is defined as:

$$J^3 = \begin{bmatrix} l_1 \sin\theta_1 & l_2 \sin\theta_2 & l_3 \cos\theta_3 & -l_4 \cos\theta_4 \\ l_1 \sin\theta_1 & l_2 \sin\theta_2 & l_3 \sin\theta_3 & l_4 \sin\theta_4 \end{bmatrix} \quad (13)$$

The Moment-Based Cost Function (MCF) presented in [14,16] is likely derived using the Newton-Euler method. The MCF is a measure of the system's performance, and it can be used to optimize the design or control parameters of the mechanism for efficient stair climbing.

In the dynamic model formulated using the Newton-Euler method, external forces applied to the system are considered. Specifically, the force applied to the foot by the pedal is an essential external force that needs to be accounted for.

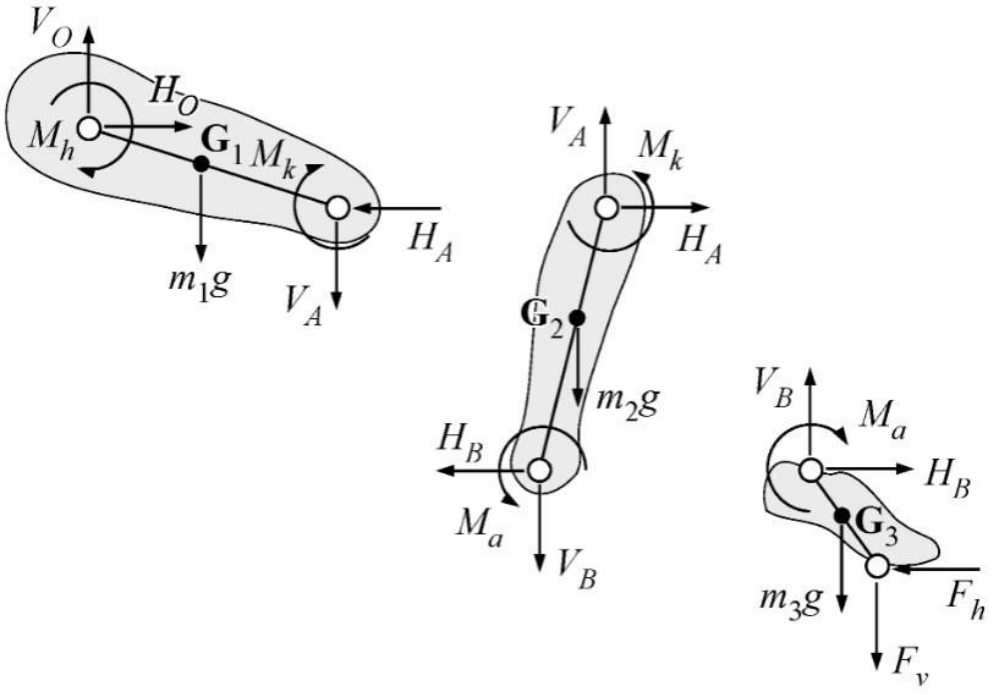

Figure 8. Free body diagram for the Newton–Euler formulation

In Figure 8, the free body diagram of the leg is shown, which is used to formulate the dynamic model using the Newton-Euler method. The forces acting on the leg include the horizontal and vertical components of the pedal force, denoted as Fh and Fv, respectively.

$$F_e = F_0 + \sum_{\P=3}^{3} F_{\P} s^{a} \mathrm{V} n(\varphi + \beta^{a} \mathrm{V}) \tag{14}$$

To calculate these components, the fitting law (14) of the forces and is used. The fitting law likely represents an empirical relationship based on experimental data or other considerations that model the forces applied to the foot by the pedal. The first two equations of the system (15) express the horizontal and vertical components of the pedal force as a function of the forces and . These equations are used to determine the external forces acting on the leg during the stair climbing motion. The inclusion of external forces, such as the pedal force, is crucial in the Newton-Euler method as it enables a comprehensive analysis of the forces and torques acting on the mechanism. By considering external forces, the dynamic model can accurately describe the interactions between the mechanism and the environment, leading to a more accurate representation of the system's behavior during stair climbing.

$$\begin{gathered} F_h = F_r s^{a} \mathrm{V} n\varphi + F_e cos\varphi \\ F_v = F_r cos\varphi - F_e s^{a} \mathrm{V} n\varphi \\ H_B = m_3 a_{G3x} + F_h \\ = {}_3(\ + \ {}_3) + \\ = {}_2 \ {}_2 + \\ = {}_2(\ + \ {}_2) + \end{gathered} \tag{15}$$

$$M_a = -I_{G_3}\theta_3 - (F_v s^{a} \mathrm{V} n\theta 3 + F_h cos\theta 3) l3 - m_3(g s^{a} \mathrm{V} n\theta 3 - a_{G3x} cos\theta 3 - a_{G3y} s^{a} \mathrm{V} n\theta 3) p_3$$

$$M_k = M_a + I_{G_2}\theta_2 + (V_B s^{a} \mathrm{V} n\theta 2 + H_B cos\theta 2) l2 + m_2(g s^{a} \mathrm{V} n\theta 2 - a_{G2x} cos\theta 2 - a_{G2y} s^{a} \mathrm{V} n\theta 2) p_2$$

$$M_h = -M_k - I_{G_1}\theta_1 - (V_A s^{a} \mathrm{V} n\theta 1 + H_A cos\theta 1) l1 - m_1(g s^{a} \mathrm{V} n\theta 1 - a_{G1x} cos\theta 1 - a_{G1y} s^{a} \mathrm{V} n\theta 1) p_1$$

Deriving from 16, the MCF cost function, based on the average absolute lower extremity joint moments, can now be defined as:

$$= \frac{1}{2} \int_{0}^{2} \left(\frac{|Ma| + |Mk| + |Mh|}{3} \right) \tag{16}$$

Cycling activity has a different cycle of movement than the walking cycle. During cycling, the term gait cycle is used instead of the pedal cycle. Here are the general stages of the pedal cycle during cycling:

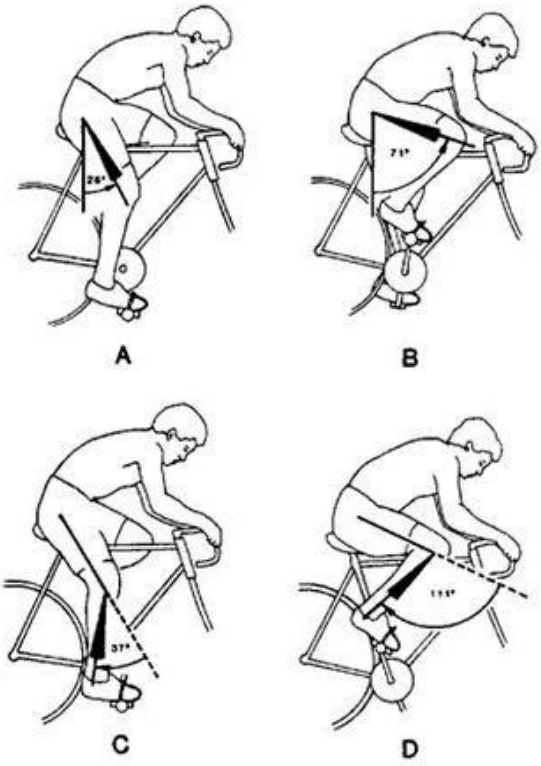

Figure 9. The General Stages of The Pedal Cycle During Cycling

- Pedal Start: The start of the pedal cycle is the point where the pedal is at its lowest point. At this point the legs are usually slightly bent and the muscles that will generate the push of the pedal are activated.
- Push Phase: The push phase is the stage where the leg pushes the pedal down. During this phase, the muscles (quadriceps, gluteus, and hamstrings) are activated and pushing the pedal down makes the bike move forward. The push phase is the phase where the most force is applied and the most power is produced.
- Bottom Point: At the end of the pushing phase, the pedal reaches the bottom point. At this point the legs are usually completely straight and represent the position where the pedal is fully pushed.
- Pulling Phase: In the pulling phase that starts after the lower point, the legs pull the pedal backwards. At this stage, the hamstring muscles are activated and allow the pedal to move backwards. The pull phase brings the leg back to the preparation position and provides energy to move to the next pushing phase.

- Top Point: At the end of the pulling phase, the pedal moves upwards and reaches the top point. At this point the legs are slightly bent in preparation for the start of the next pedal cycle.

Cycling activity continues as a continuous cycle of pedals. The push, pull, bottom and top stages are repeated continuously. Cyclists continuously perform the pedal cycle, ensuring constant movement and progress. Pedal cycling during cycling requires the coordination and strength of leg muscles. Cyclists effectively perform every stage in the pedal cycle, ensuring an efficient and powerful ride.

The volunteer initiates the movement while seated, as depicted in Figure 10. Both feet are placed on the pedals of the bicycle, which is adjusted to provide a consistent minimum level of resistance for all participants. Throughout the movement, the upper body remains stable and stationary.

Figure 10. Cycling

The cycling motion takes place in the sagittal plane, as illustrated in Figure 10. To define a complete cycle for this movement, a marker located on the calcaneus is used as a reference. The marker should complete one full rotation, returning to its initial position, to complete a single cycle.

2.3. Material

In this section, the materials that are used in the study is explained in detail. By providing a comprehensive overview of the materials used in the study, readers can better understand the setup and methodology employed, thus ensuring transparency and reproducibility of the research.

2.3.1. Force Sensor for Biomechanical Simulations of a Cycling Activity

Accurate data collection is essential in biomechanical modeling to effectively study and analyze activities. While motion capture systems are commonly used for capturing kinematic information, they are not suitable for measuring kinetic inputs like reaction forces in cycling activities. Traditional force plates fixed to the ground in gait laboratories cannot accurately measure forces occurring at the surface of the saddle and pedals. Therefore, a portable force plate is needed. One of the common methods for measuring pedal forces is through the use of load cells. Load cells are affordable and easy-to-use devices that sense and measure forces and moments. The most widely used type of load cell is the strain gauge load cell. These load cells consist of thin foil resistors attached to different metals, which act as the sensing elements. When a force is applied, the strain gauge deforms, causing a change in electrical resistance. This change in resistance can be correlated to the applied force. By accurately measuring the pedal forces using strain gauge load cells, it becomes possible to calculate the torque exerted by multiplying the crank distance. Although commercial power meters are available for estimating torque, they are often expensive and not easily accessible to many researchers and practitioners.

In this particular study, the researcher developed an in-house force sensor using strain gauges in a Wheatstone bridge configuration. The sensor had a maximum capacity of 100 kg. When a force was applied to the strain gauges, it caused a change in electrical resistance, resulting in a modified electrical signal. To process the signals from the strain gauges, the researchers utilized the HX711 Weighing Sensor module, which included a 24-bit analog-to-digital converter (ADC) chip. This module amplified the low electric output from the strain gauges and converted the analog signal into a digital format for further analysis. The amplified and converted signal was then sent to a microcontroller, such as Arduino, to obtain weight or force information. Overall, the researchers

successfully developed a force sensor using strain gauges and a Wheatstone bridge configuration. The HX711 module played a crucial role in amplifying and converting the electrical signals, while the microcontroller facilitated the processing and interpretation of the force data obtained from the sensor.

2.3.1.1. Calibration

Calibration of the load cell involves reading and setting the zero (tare) value, which is then calibrated to a known mass value. This calibration process ensures that the load cell provides accurate measurements by calibrating it with a known mass each time it is utilized, thus providing the best estimate for the mass of objects with unknown masses.

The calibration was performed under the assumption of linearity using Equation 18. This equation represents a line and was implemented with an Arduino board and the load cell. By establishing this linear relationship, the load cell can accurately convert measured values into corresponding mass values.

$$= \quad + \tag{18}$$

In the calibration equation, the reading from the HX711's ADC is denoted by x, the known mass is represented by y, the slope of the calibrated line is indicated as m, and the intercept where y equals zero (the "tare" point) is denoted by b. These variables collectively define the relationship between the ADC reading and the corresponding mass, allowing for accurate mass estimation based on the load cell measurements.

Indeed, if dummy points x0, y0 are utilized as one point on the line, and x1, y1 are used as the second point on the line, both the slope (m) using Equation 19 and intercept (b) can be defined in terms of the known masses and ADC values.

$$m = \frac{y_1 - y_0}{x_1 - x_0} \tag{19}$$

Indeed, when the load cell measures zero weight, the corresponding ADC reading is also zero. Therefore, in the expression mentioned earlier, the value of y0 is zero. This simplifies the expression(20) as follows:

$$y = \left(\frac{y_1}{x_1 - x_0}\right)(x - x_0) \quad (20)$$

The linear correlation between strain and the applied force enables us to employ a linear calibration method for the load cell.

2.3.1.2. Static Test

The force sensor's behavior under static loads was examined using standard loads of 1000, 1200, and 1500 grams. Each load was placed on the sensor three times and left for 5 seconds. The resulting data was saved in an .xlsx file. Bland-Altman agreement analysis (α=0.95) was conducted by averaging the three repetitions to assess the agreement between the standard loads and the force plate data.

2.3.1.3. Dynamic Test

In order to investigate the behavior of the force plate under dynamic loads, it was attached to the right pedal of a bicycle. The left pedal was equipped with a power meter pedal (Favero Assioma UNO). The study obtained ethical approval from the Izmir Ataturk Research and Training Hospital for conducting in vivo tests. A 44-year-old subject, weighing 70.8 kg and measuring 180 cm, participated in the experiment. After a 3-minute warm-up, the saddle height was adjusted according to the subject's anthropometry. To capture and extract pedal power data, the information from the power meters was transmitted to a computer using Zwift software (Zwift Inc., California, US). The subject connected the pedals to Zwift via Bluetooth, configuring them as a power meter, which allowed for the automatic recording of movement and force values when the cyclist pressed the pedals.

During the experiment, the subject synchronized the activation of the load cell and the pedal power meters. The subject cycled at their own pace for a duration of 30 seconds while remaining seated on the saddle. This procedure aimed to capture relevant data regarding the forces exerted on the pedals and the corresponding power output.

2.3.1.4. Validation

During the pedaling motion, the rotation of the crank ideally occurs in a two-dimensional plane. The crank's angular position is determined by the circular trajectory of a point on the crank, excluding the pivot point. Similarly, if a point on the pedal is located on the pedal's pivot point, its trajectory can be used to calculate the angular position. The total force applied to the pedal, denoted as total, is the combination of vector forces generated by the contractions and extensions of the leg and hip muscles. These forces can be divided into normal force (n) and shear force (s), as shown in Figure 11. The normal force n is perpendicular to the surface of the force platform, while the shear force s is parallel to the surface. The perpendicular components of these forces create a torque around the pivot point of the pedal crank arm.

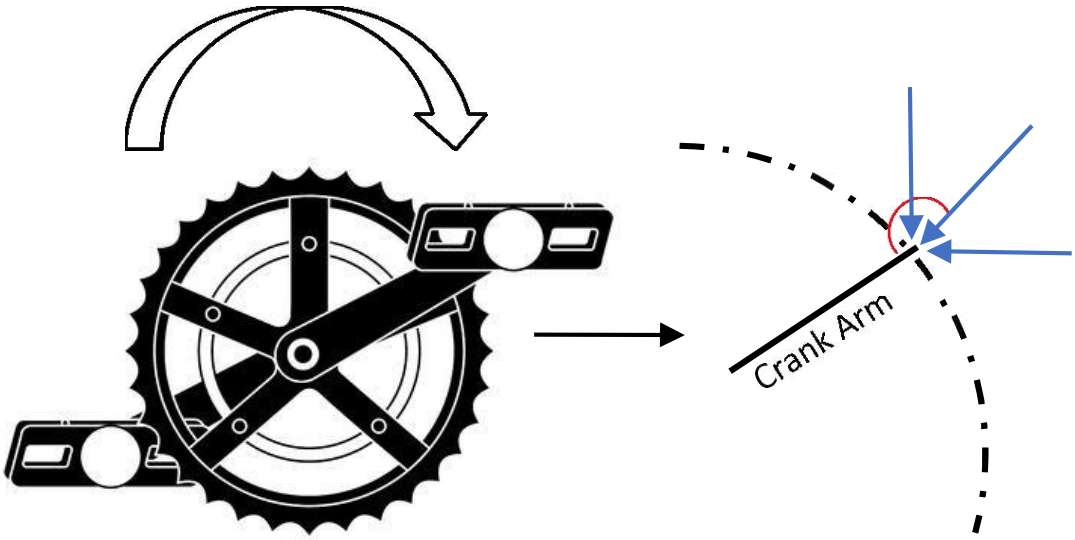

Figure 11. Free Body Diagram of the Pedal

$$\vec{F}_{total} = \vec{F}_n + \vec{F}_s \tag{21}$$

The torque, in the context of pedal motion, refers to the rotational effect produced by a force applied to the pedal pivot point around the axis defined by the bearing. Mathematically, torque can be calculated as the cross product of the lever-arm length vector and the force vector. The lever-arm length vector represents the distance from the axis of rotation (pedal pivot point) to the line of action of the force, while the force vector represents the magnitude and direction of the applied force. By taking the cross product

of these two vectors, the torque exerted on the pedal pivot point can be determined, providing insight into the rotational motion of the pedal.

$$\|r\| = \|\vec{L}_c \; x \; \vec{F}_{tota} \quad \| = \qquad \tan(\;) \qquad (22)$$
$$F_{total}$$

: Torque (N.m)

: Level arm (m)

: Normal component of resultant force (N)

: Total force (N)

: Angle between and (in radians)

Torque is a quantification of the rotational effect produced by a force applied to an object. It determines the extent to which the force induces rotation. The power generated by torque is determined by multiplying the torque value by the rotational speed, also known as cadence. In this way, the resultant force can be calculated using the following formula:

$$(\;) = \frac{Power(watts)}{(candance(rpm)\; x \frac{2\; x\; \pi}{60(\qquad)}) * L_c(meter)} \qquad (23)$$

To compare the power output measured by power meter pedals (Favero Assioma UNO) with the force sensor output, the power data recorded by the pedals are converted into force using Equation (23). After this conversion, the outputs obtained from both measurement methods are subjected to Bland-Altman agreement analysis with a confidence level of 95 percent (α=0.95) [23]. This analysis is used to assess the level of agreement between the two measurement techniques.

The Bland-Altman agreement analysis is a statistical method that allows researchers to examine the agreement between two measurement methods by plotting the difference between the measurements against their average. It provides insights into the bias between the methods (i.e., whether one method consistently measures higher or lower) and the limits of agreement (i.e., the range within which most of the differences lie). This analysis is valuable for understanding the consistency and accuracy of the measurements provided by the two different techniques.

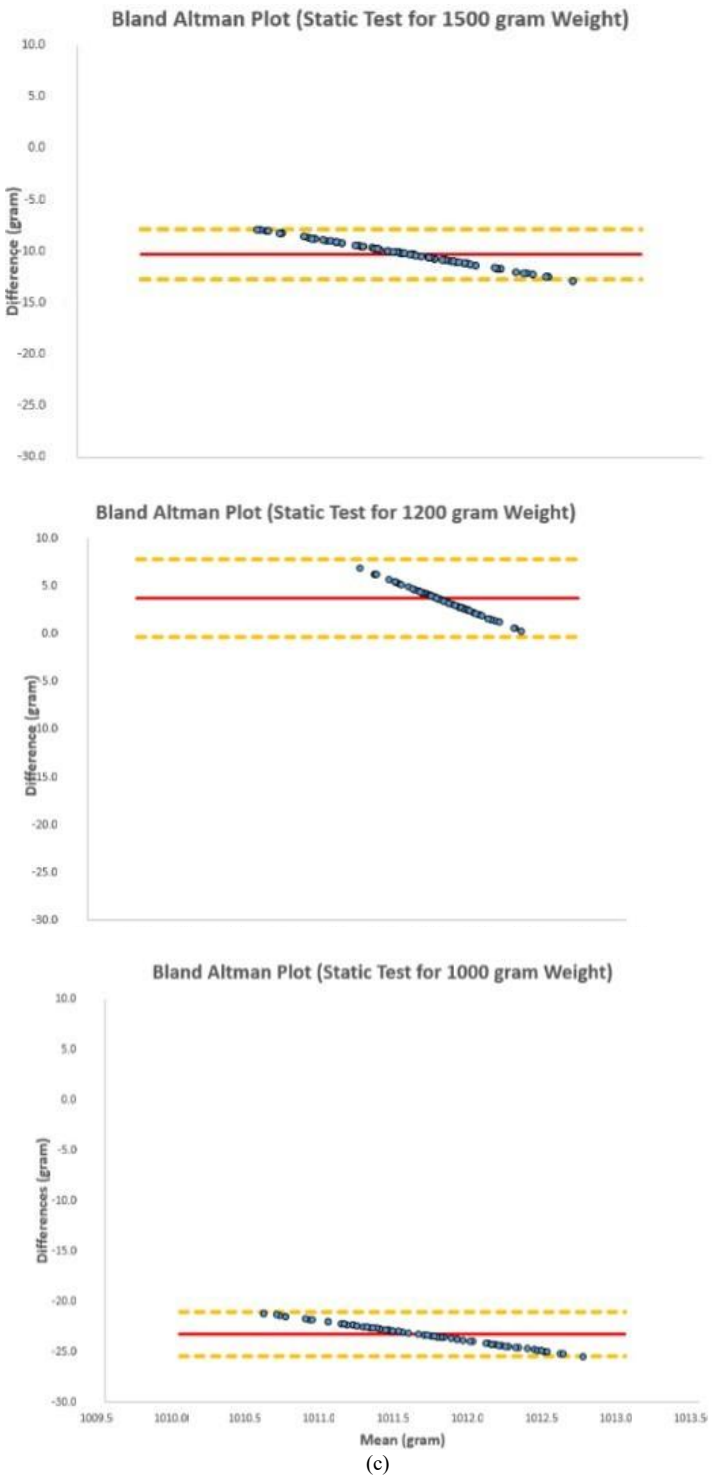

(c)

Figure 12 a) Bland Altman Plot for Static Test (Static Test for 1500 g Weight),
b) Bland Altman Plot for Static Test (Static Test for 1200 g Weight),
c) Plot for Static Test (Static Test for 1000 g Weight)

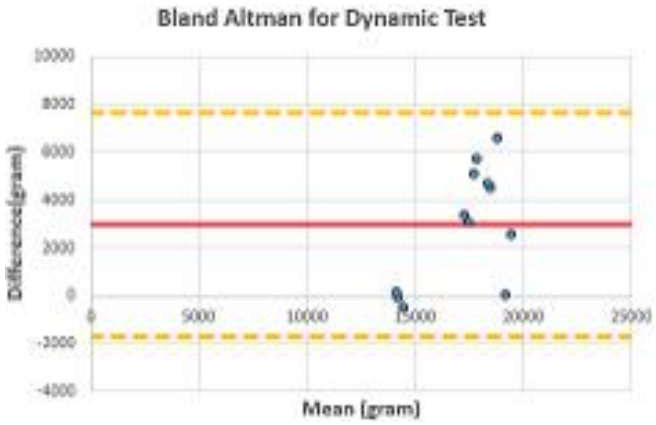

(a)

		Bland Altman Analysis	
		Bias (g)	SD Bias (g)
Static Test	1500 g	10	1
	1200 g	3	2
	1000 g	23	1
Dynamic Test	12 cycles	2327	1910

(b)

Figure 13. a) Bland Altman Plot for Dynamic Test (12 cycles)
b) Bland Altman Analysis of Tests

Table 3. Average Values of Static Loads

	Trail 1		Trail 2		Trail 3	
Loads	Average (g)	STD (g)	Average (g)	STD (g)	Average (g)	STD (g)
1000 g	1023	11	1024	15	1022	17
1200 g	1196	21	1198	15	1198	15
1500 g	1510	13	1511	14	1510	11

Table 3. displays the average values and standard deviations for each trial. The deviation within each trial is approximately 0.1% for both the load and the pedal power meter measurements. The results of the dynamic test for 12 cycles show a value of 18752 ± 2755 g for the pedal power meter, while the force sensor measurement yields 15790 ± 1449 g. In Table 3. the results of the Bland-Altman analysis are presented. The mean differences and standard deviations for the static tests indicate low variability between the measurements. However, for the dynamic test, both the mean difference and standard deviation are relatively high, suggesting greater variability between the measurements in this particular test. Figure 14a-b. illustrates the body model and its corresponding output.

The force sensor is designed to serve as an input for the biomechanical modeling software, AnyBody (AnyBody Technology A/S, Aalborg, Denmark). The force sensor measurement is integrated into AnyBody using an XML file, and the force vector is identified on the metatarsal 2 bone, as shown in Figure 14a. This successful integration demonstrates that the force sensor can be effectively utilized within the biomechanical modeling software.

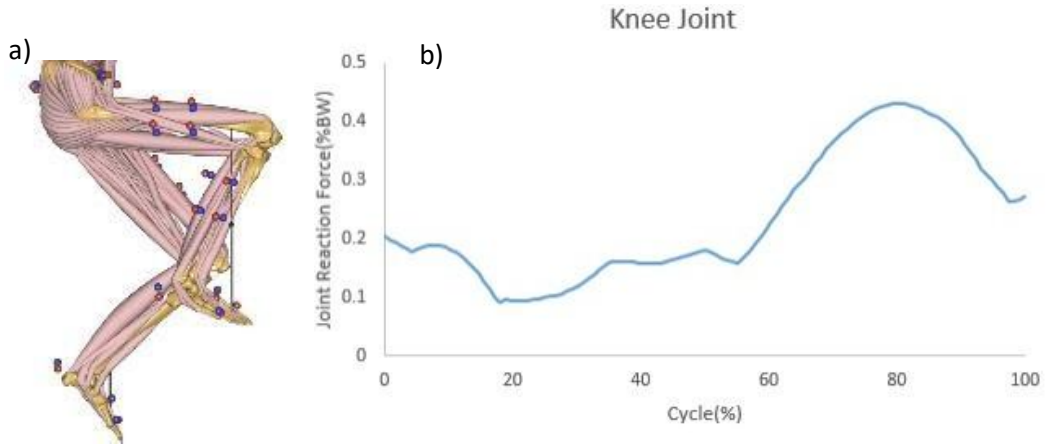

Figure 14. a) AnyBody Model , b) Anteroposterior Reaction Force (Vertical) of Knee Joint

The study indicates that the force sensor delivers accurate and precise measurements under static loads. As a suggestion for future research, the development of a force sensor capable of measuring shear forces during a pedal stroke could be pursued. In this particular study, a cost-effective and custom-made sensor was successfully employed to simulate cycling activity within a biomechanical simulation program. This approach yielded realistic results by effectively incorporating environmental interactions. The successful demonstration of this sensor highlights its potential for practical applications in biomechanical simulations at an affordable cost.

2.3.2. Qualisys Motion Capture System

Qualisys, a renowned motion capture (MOCAP) system based in Gothenburg, Sweden, offers a highly accurate and reliable solution for in vivo studies. Their flagship product, Qualisys Track Manager (QTM), is specialized tracking software designed to efficiently capture precise data from models. This software enables real-time collection

of both 2D and 3D coordinates (X, Y, and optionally Z) at a sampling rate of 100 Hz, providing six degrees-of-freedom information.

The Qualisys motion capture system includes eight Miqus3 cameras, which are strategically placed to capture the motion from multiple angles (see Figure 18). These cameras, with a resolution of 1824x1088 pixels in 2D and an impressive 0.11 mm resolution in 3D, cover a volumetric space of 10 cubic meters. Additionally, there is one Miqus Video Camera and a set of 50 Super Spherical Markers with a diameter of 14 mm (see Figure 15). These markers, equipped with a reflective surface, play a vital role in the motion capture process. They reflect light back to the cameras, allowing the formation of the marker's image. It is crucial to maintain an unobstructed line of sight between the cameras and the markers to ensure accurate tracking. If a marker is not visible to any camera at a given time, its position cannot be detected. To address this, the QTM software employs an automatic extrapolation method to fill in any gaps caused by temporary marker occlusion. However, it's important to note that extrapolated data may not always accurately represent the true motion. Therefore, maintaining a continuous line of sight between the cameras and markers is essential for reliable tracking results.

Figure 15. Miqus M3 Camera and Reflective Markers

In addition to the Qualisys system components, the setup also includes the DELSYS TRIGNO AVANTI 4 Channeled Wireless Surface EMG system from Delsys, Massachusetts, USA, and a portable force platform from BERTEC in Quincy, USA. These supplementary devices enable the capture of electromyography (EMG) data and measurement of ground reaction forces, respectively. Overall, the Qualisys motion capture system, with its advanced hardware and software components, provides researchers with a powerful tool for collecting precise and fast motion data in vivo. The system's high accuracy, real-time capabilities, and integration with specialized analysis software like OpenSim and Visual 3D Gait Analysis make it a valuable.

Table 4. Qualisys (Goteborg, Sweden) Specifications

Qualisys (Goteborg, Sweden) Specifications	
Normal Mode	2 MP (340 fps)
Hİ-Speed Mode	0.5 MP (650 fps)
Resolution	1824x1088
3D Resolution	0.11 mm
Max. Capture Distance	15 m
Standart Lens	64x41˚
Wide Lens	80x53˚
Narrow Lens	44x27˚
Sampling Rate	100 Hz
Software	Qualisy Track Marker
Marker Size	Ø14 mm
Calibration Wand Length	301.4 mm

Calibrating the Qualisys system is an essential procedure that must be performed prior to data collection. This calibration process establishes the reference coordinate axis and defines the workspace, ensuring accurate and reliable tracking of markers. Regular calibration of the Qualisys system is recommended to maintain optimal marker tracking performance. The calibration is carried out using the system's calibration kit, which consists of a carbon fiber calibration wand with a precise length of 301.4 mm and an aluminum L-frame.

To facilitate effective marker tracking during experiments, the Miqus M3 cameras are strategically positioned in the laboratory. They are mounted in pairs of three on the left and right walls, placed at a height of 2 meters from the ground. Additionally, two cameras are placed at the laboratory corner to enhance the line-of-sight for marker tracking. The video camera, on the other hand, is mounted on the right wall, positioned at a height of 1 meter from the ground. Its placement allows clear visibility of the force platform located at the center of the podium in the laboratory.

The BERTEC portable force platform (manufactured in Quincy, USA) is utilized for the collection of ground reaction force data from the volunteers, serving as a valuable resource for the kinetics component of the project. The force platform, with dimensions of 600 x 400 x 50 mm, is positioned at the center of the gait path. It is equipped with 16 digital channels that enable the measurement of forces and moments occurring along each

axis. This comprehensive setup allows for the precise capture and analysis of forces and moments exerted during various movements and activities.

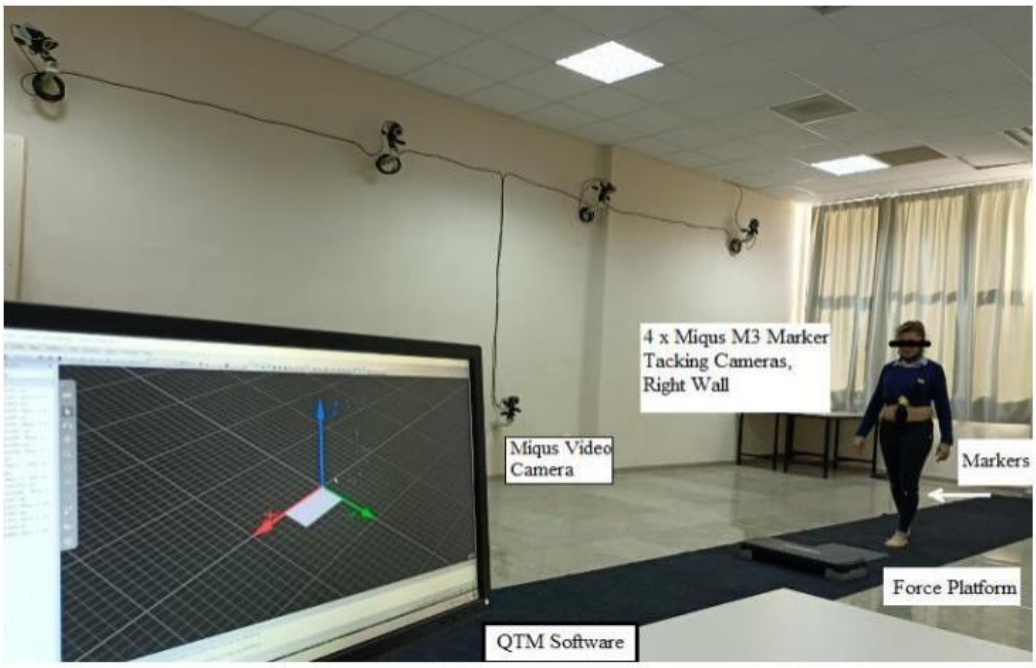

Figure 16. Biomechanics and Motion Capture Systems Laboratory

2.3.3. OpenSim and AnyBody Analysis Software

OpenSim and AnyBody Analysis Software are both widely used software tools in the field of biomechanics for analyzing human movement and studying musculoskeletal systems. While they serve similar purposes, there are some differences between the two.

2.3.3.1. OpenSim

OpenSim is an open source software platform used in medicine, sports science and biomechanics. It is used to analyze human movement and dynamics of the musculoskeletal system. It was developed by the National Rehabilitation Research Simulation Center (NCSRR) at Stanford University.

OpenSim has the following key features:

- Biomechanical Modeling: OpenSim allows you to create detailed biomechanical models of the human body including muscle, bone, joints and other tissues. These models are created based on real human anatomy and are used in motion analysis.

- Motion Simulation: OpenSim simulates the interactions of muscles on the musculoskeletal system. These simulations are used to predict muscle activations, joint forces, muscle strengths, and other movement variables.
- Analysis Tools: OpenSim enables users to perform biomechanical analysis. These analyzes include patterns of muscle activation, joint moments, forces at joints, muscle power output, and other kinematic and kinetic parameters.
- Customization and Extensibility: OpenSim has a customizable and extensible structure according to users' needs. Users can configure OpenSim as they wish and create new analytics, models and simulations through its API and scripting features.
- Community and Source Code Access: OpenSim has a large user community and an open source development model. Users can access the source code, fix bugs, add new features, and collaborate with the OpenSim community.

2.3.3.2. AnyBody Analysis Software

AnyBody Analysis Software is a commercial software package used for biomechanical analysis. It was developed by the Swedish company AnyBody Technology.

AnyBody Analysis Software has the following key features:

- Human Modeling: AnyBody Analysis Software provides comprehensive tools for human body modeling. You can create detailed and realistic models containing bones, muscles, joints and other anatomical structures.
- Motion Simulation: AnyBody offers advanced simulation capabilities for kinematic and dynamic analysis. These simulations are used to estimate muscle activations, joint moments, muscle strengths and other movement parameters.
- Optimization: AnyBody can automatically adjust model parameters with optimization algorithms. This can be used to align with experimental data or to achieve specific goals.
- Analysis Tools: AnyBody offers a variety of analysis tools. These tools include muscle activation analysis, joint reaction force calculations, muscle function analysis, and energy expenditure assessments.

- Integration: AnyBody can be integrated with other software and hardware tools. For example, integration with motion capture systems, force platforms and EMG systems can be achieved.

AnyBody Analysis Software is a comprehensive tool used in various fields such as biomechanical research, product design and physical rehabilitation. Once the body segments are defined within OpenSim or AnyBody, researchers can conduct kinematics and kinetics calculations on these segments. This includes analyzing joint angles, segmental velocities, accelerations, forces, and moments during the selected activities. These calculations provide valuable insights into the biomechanical aspects of human movement and help in understanding the underlying mechanisms involved.

2.4. Methodology and Data Collection

In this section of the thesis, a comprehensive explanation of the methodology and data collection process is provided. The methodology encompasses the timeline of volunteer activities, while the data collection process involves capturing data from the gold standard motion capture system and post-processing it. The flowchart in Table 8 outlines the step-by-step procedure, commencing with the preparation of the volunteers. To conduct the experiment effectively, daily life activities are treated as separate modules within the Qualisys Track Manager software due to the use of different modules for analysis.

By providing a comprehensive explanation of the methodology and data collection process, the thesis aims to ensure clarity and reproducibility, allowing other researchers to understand and replicate the study's procedures accurately. The use of a gold standard motion capture system and thoughtful data organization contribute to the overall robustness and reliability of the study's findings.

A total of 10 volunteers from the Mechanical Engineering Department of Izmir Institute of Technology participated in the daily life activities. The volunteers' characteristics were recorded, including age (22 ± 2), height (1.69 ± 0.13 m), and weight (62.5 ± 15.5 kg) for the stair climbing and cycling. The experiments were conducted under the guidance of two qualified physiotherapists. These professionals were responsible for measuring the volunteers' body segments and accurately placing the reflective markers on the appropriate anatomical locations. This meticulous process was crucial to establish

accurate segment models and minimize user-based errors. However, since multiple physiotherapists were involved in marker placement, differences may have arisen. To assess the reliability between the two physiotherapists, the absolute mean differences of joint angles and the coefficient of determination (R2) values were calculated.

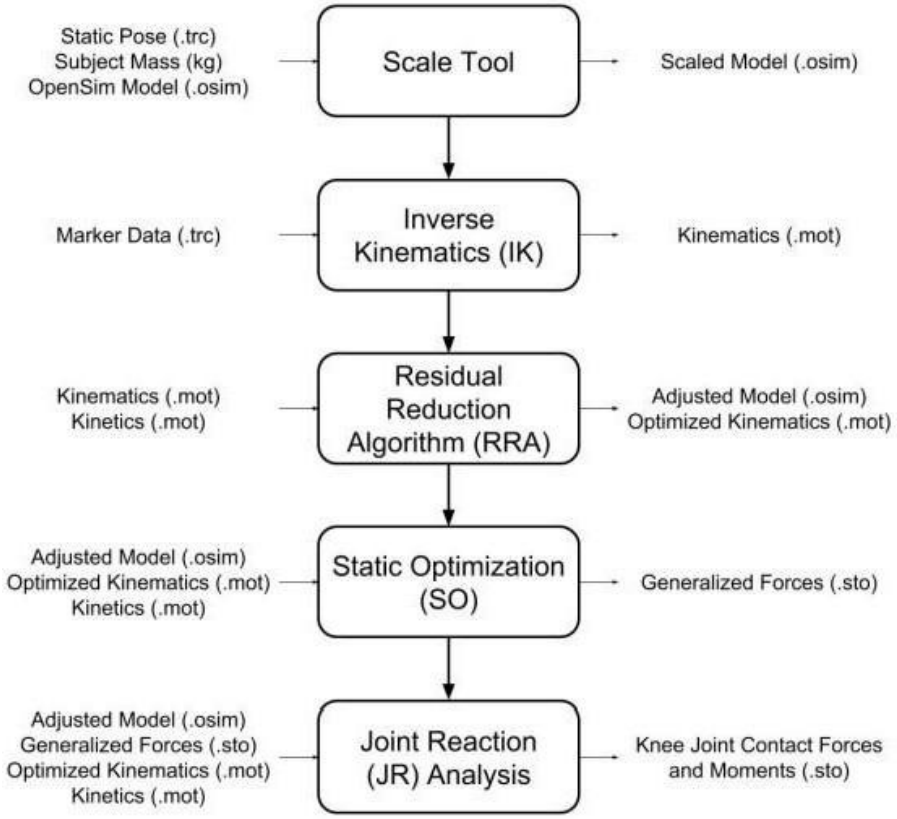

Figure 17. Methodology and Data Collection Diagram For OpenSim

Intra-tester reliability tests were performed on three volunteers by the two physiotherapists. Joint angles at heel strike and toe-off moments in the sagittal plane, specifically for the hip, knee, and ankle joints, were examined by calculating mean angles and standard deviations. The coefficient of determination (R2) was then determined using linear fitting. Ranging from 0 to 1, the R2 value indicates the degree of agreement, with 0 representing a lack of agreement and 1 indicating a perfect fit. The joint angles in the sagittal plane yielded results smaller than 5°, which aligns with the reported minimal detectable changes in gait kinematics. The calculated R2 values were 0.98 for the hip joint, 0.96 for the knee joint, and 0.90 for the ankle joint (Mihçin et al., 2023). Prior to the volunteers' participation in the activities, several measurements were taken to gather data on their body segments, weight, and height. These measurements

encompassed various parameters, including pelvis-medial, knee width, ankle width, sole delta, leg length, wrist width and thickness, elbow width, arm length, and shoulder offset. Ensuring consistency in these measurements was crucial since the same data would be utilized in another part of the project that pertained to kinetics.

Subsequently, the volunteers were prepared for data collection using the Qualisys gold standard motion capture system. To establish the laboratory axes, a calibration process was conducted employing a calibration kit. This kit involved the use of a T-shaped wand equipped with markers on both ends, enabling the definition of the workspace volume. Additionally, an L-frame positioned at the laboratory's center aided in establishing the laboratory axes. The construction of the workspace volume was done meticulously to ensure optimal line-of-sight for the cameras, enabling the accurate capture of the markers (refer to Figure 18).

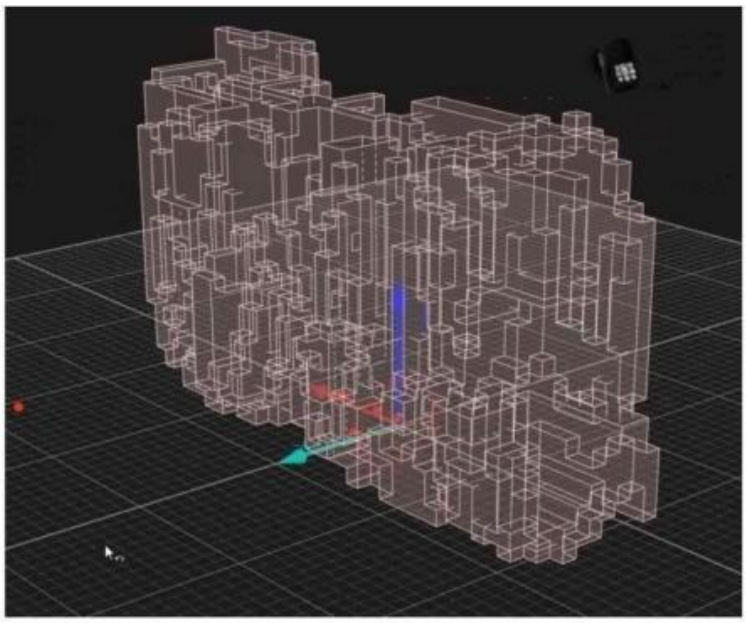

Figure 18. Calibrated Workspace Volume

After successfully completing the calibration of the workspace, the volunteers are then prepared for data collection. This involves the precise placement of reflective markers onto specific anatomical locations of the volunteers' bodies. This step is crucial because the retro-reflective markers of the Qualisys motion capture system are essential for tracking human motion and conducting subsequent analyses. Thanks to the expertise of the physiotherapists, the anatomical landmarks are accurately identified, and the markers are carefully placed. The placement of markers follows the guidelines provided

by the CAST Dynamic Full Body Marker Set and CAST Static Full Body Marker Set, which are clinically proven marker sets defined by the International Society of Biomechanics (ISB) (refer to Figure 19). These marker sets have been specifically chosen for this study to ensure consistent and accurate tracking during activities of daily living (ADLs) , while also minimizing any potential line-of-sight issues.

Table 5 and 6 define the anatomical landmarks of the body where markers are placed.

In this study, the marker setup includes two sets of markers: the static marker set and the dynamic marker set, with a specific focus on the lower body region. The static marker set consists of eight additional markers placed at specific locations, such as the lateral and medial epicondyles (L_FLE, L_FME, R_FLE, R_FME) of the femur, as well as the lateral prominence of the lateral malleolus and medial prominence of the medial malleolus (L_FAL, L_TAM, R_FAL, R_TAM). These extra markers, known as static markers, serve the purpose of creating a static model of the body in software applications like OpenSim and Anybody, which involves building thigh, shank, and foot bones. Once the static pose is recorded using the static markers, they are subsequently removed. The removal of the static markers does not cause any calculation issues or distort the data for the dynamic model since the segments of the legs are tracked using other markers (R_TH1, R_TH2, R_TH3, R_TH4, R_SK1, R_SK2, R_SK3, R_K4) in the dynamic marker set.

For each participant, a separate profile is created in the Qualisys Track Manager (QTM) to facilitate gait analysis and daily activity recordings. A session is initiated to record the participants' movements, and two static poses (anterior and posterior) are captured for each subject.

To ensure the accuracy of the recorded static poses, the number of markers in the computer interface is counted. If the marker count matches 55 in these static poses, it confirms that the static poses have been correctly recorded. After the static pose recordings, the volunteers then proceed to perform activities of daily living (ADLs) as part of the data collection process.

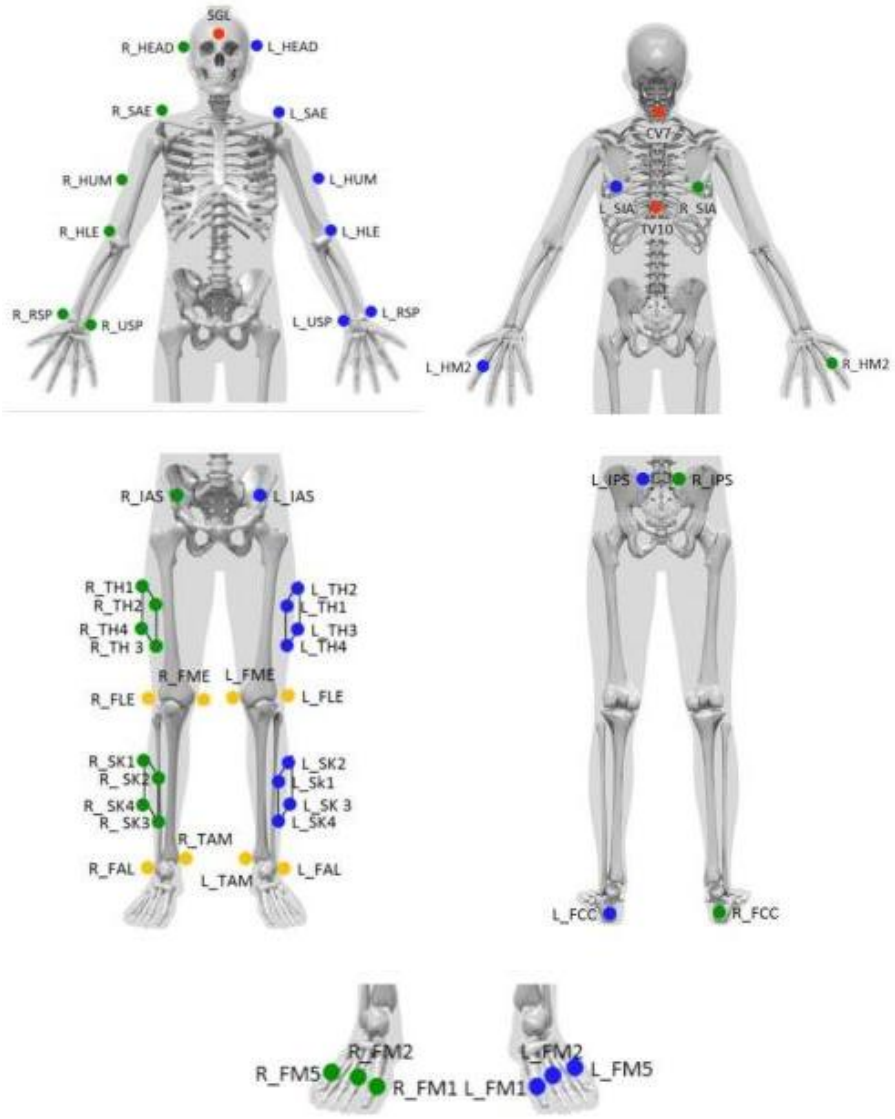

Figure 19. CAST Upper and Lower Body Marker Set

(Cappozzo et al., 1995)

Table 5. CAST Upper Body Marker Set List

(Source: Sint Jan et al., 2007)

Name	Ref.	Location	Static	Dynamic
L_HEAD		Just above the ear	X	X
R_HEAD		Just above the ear	X	X
SGL	SGL	Glabulla	X	X
CV7	CV7	Cervical Vertebrae	X	X
L_SIA	SIA	Scapula-İnferior Angle	X	X
R_SIA	SIA	Scapula-İnferior Angle	X	X
TV10	TV10	Thoracic- Vertebrae	X	X
L_SAE	SAE	Scapula-Acromial Edge	X	X
L_HUM			X	X
L_HLE	HLE	Humerus-Lateral Epicondyle	X	X
L_RSP	RSP	Radius-Styloid Process	X	X
L_USP	USP	Ulna- Styloid Process	X	X
L_HM2	HM2	Basis of Forefinger	X	X
R_SAE	SAE	Scapula-Acromial Edge	X	X
R_HUM			X	X
R_HLE	HLE	Humerus-Lateral Epicondyle	X	X
R_RSP	RSP	Radius-Styloid Process	X	X
R_USP	USP	Ulna- Styloid Process	X	X
R_HM2	HM2	Basis of Forefinger	X	X

Table 6. CAST Lower Body Marker Set List

(Source: Sint Jan et al., 2007)

Name	Ref.	Location	Static	Dynamic
L_IAS	IAS	Anterior superior illiac spine	X	X
L_IPS	IPS	Posterior superior illiac spine	X	X
R_IAS	IPS	Posterior superior illiac spine	X	X
R_IPS	IAS	Right anterior superior illiac spine	X	X
L_TH1-4		Cluster	X	X
L_FLE	FLE	Lateral epicondyle	X	
L_FME	FME	Medial epicondyle	X	
L_SK1-4		Cluster	X	X
L_FAL	FAL	Lateral prominence of the lateral malleolus	X	
L_TAM	TAM	Medial prominence of the lateral malleolus	X	
L_FCC	FCC	Aspect of the Achilles tendon insertion on the calcaneus	X	X
L_FM1	FM1	Dorsal aspect of the first metatarsal head	X	X
L_FM2	FM2	Dorsal margin of the second metatarsal head	X	X
L_FM5	FM5	Dorsal margin of the fifth metatarsal head	X	X
R_TH1-4		Cluster	X	X
R_FLE	FLE	Lateral epicondyle	X	
R_FME	FME	Medial epicondyle	X	
R_SK1-4		Cluster	X	X
R_FAL	FAL	Lateral prominence of the lateral malleolus	X	
R_TAM	TAM	Medial prominence of the lateral malleolus	X	
R_FCC	FCC	Aspect of the Achilles tendon insertion on the calcaneus	X	X
R_FM1	FM1	Dorsal aspect of the first metatarsal head	X	X
R_FM2	FM2	Dorsal margin of the second metatarsal head	X	X
R_FM5	FM5	Dorsal margin of the fifth metatarsal head	X	X

2.5. Postprocessing of the Data

The postprocessing of the collected data begins by properly labeling the reflective markers in the Qualisys Track Manager (QTM) software. This step is crucial for accurate analysis, as mislabeled markers can have a significant impact on the results. The markers are labeled according to the chosen CAST Marker Set, which provides a standardized approach for marker placement. Initially, the static pose data is labeled to establish a baseline for the subsequent dynamic labeling. Dynamic labeling is then performed on the collected activities of daily living (ADLs) . Another important step in the postprocessing phase is the identification of all markers. In cases where line-of-sight issues occur during the activity, missing marker periods need to be filled using appropriate extrapolation methods. QTM offers several extrapolation methods, including static, linear, polynomial, relational, virtual and kinematic methods. In this thesis, several extrapolation methods are used to address missing marker data and maintain the continuity and completeness of the recorded motion. The most commonly employed extrapolation methods include linear, polynomial, relational, and virtual methods. The relational extrapolation method is specifically applied to fill gaps between two frames when a marker is missing. This method relies on the position of other markers to extrapolate the missing marker's position. It involves using one marker to define the origin, another marker to define the x-direction, and a third marker to define the xy-plane for the missing marker. By establishing these relational relationships, the missing marker's position can be estimated.

Similarly, the relational extrapolation method is used for other missing markers by extrapolating their positions based on the surrounding markers' information. This method helps bridge the gaps in marker data and ensures the continuity of motion capture. On the other hand, the virtual extrapolation method is employed in cases where a marker encounters line-of-sight issues and remains invisible throughout the entire activity cycle. In such situations, a virtual marker is created in place of the missing marker to maintain the integrity of the motion data. These extrapolation methods are essential tools in dealing with missing or obscured marker data, allowing for a more complete and accurate representation of the captured motion. By leveraging the relationships between markers and creating virtual markers when necessary, the continuity of motion capture can be preserved, even in challenging line-of-sight scenarios.

After the labeling operation, a specific cycle is selected for each activity, as described in Section 2.2. This selected cycle is then exported as a C3D file, which contains three-dimensional coordinate and numeric data for the performed activities. The C3D file consolidates various parameters, including anthropometric measures, into a single file.

The exported C3D files from QTM are subsequently utilized in software such as OpenSim and AnyBody to model the body segments or skeletal models. Each activity's C3D file, along with the static pose file, is imported into the software for further analysis.

To perform inverse kinematics and dynamic analysis on the hip joint, a pipeline is developed. The pipeline serves as a customizable tool that allows for the selection of specific steps and calculations required for the modeling and analysis process. The following steps are followed within the pipeline:

- The static pose file is chosen to assign the segments according to the defined anatomical locations .
- The full body skeleton template is selected to build the model.
- All activity files to be analyzed are chosen for further processing.
- The weight and height of the volunteer are inputted into the analysis, providing essential anthropometric data.

By following this pipeline, the software can perform the necessary computations and simulations for inverse kinematics and dynamic analysis on the hip joint using the imported C3D files and relevant anthropometric information. After the files are read and analyzed using inverse kinematic and dynamic methods with a defined order for the hip joint, the resulting data is exported to separate directories for each activity. These exported results contain detailed information about the full range of motion for a complete cycle of each activity. However, the exported data may lack a concise and comprehensive overview of key measurements such as the total range of motion, mean, standard deviation, and upper-lower limits of the entire dataset. To address this issue and gain better insights from the collected data, a MATLAB code is developed. The MATLAB code is specifically designed to process the exported results, calculate the required measurements, and generate plots for each axis of the hip joint. By analyzing the complete dataset, the code can calculate the statistical parameters of interest, allowing for a more comprehensive understanding of the hip joint motion. The generated plots are particularly helpful in visualizing the hip joint's behavior and range of motion during different activities. These plots present a clear and concise representation of the data, enabling

researchers and practitioners to identify trends, patterns, and potential variations in the hip joint motion. The generated plots provide valuable tools for comparing and interpreting results, aiding in the identification of important characteristics and potential areas for further investigation or intervention.

The MATLAB code processes the data from all activities, consolidates the relevant information, and calculates the total range of motion, mean values, standard deviations, and upper-lower limits for the entire dataset. By using this code, researchers can obtain a comprehensive understanding of the overall hip joint movement patterns and variations among the participants. This process helps in better understanding the collective behavior of the hip joint during the analyzed activities and facilitates meaningful .

CHAPTER 3

RESULTS AND DISCUSSION

In this chapter, the results of the performed activities are presented, and thorough discussions are conducted based on the obtained findings. The data collected from the activities, such as daily life activities, are analyzed, and the results are systematically organized and presented.

The chapter starts by providing an overview of the analyzed data, including the sample size, demographic information of the participants, and any relevant characteristics of the collected dataset. This information sets the context for the subsequent discussions and interpretations.

Next, the chapter delves into the specific results obtained from the analysis. The findings are presented using appropriate statistical measures, such as means, standard deviations, confidence intervals, or other relevant statistical indicators. Graphs, tables, or visual representations may also be included to enhance the clarity and understanding of the results.

Overall, this chapter provides a comprehensive examination and interpretation of the results obtained from the performed activities. It aims to offer insights, draw meaningful conclusions, and contribute to the existing body of knowledge in the field.

3.1. Results of ADLs

The stair climbing and cycling activity, captured using the gold standard motion capture system, underwent thorough processing and analysis using various software tools such as Qualisys Track Manager, OpenSim, AnyBody, and custom MATLAB code. The inverse kinematic analysis was performed using OpenSim and AnyBody, utilizing the C3D files containing comprehensive information about the collected data from the volunteers. To determine the range of motion (ROM) values for each axis of the hip joint in each activity, the maximum and minimum joint angles were extracted from the data. These extreme values represented the endpoints of the hip joint motion during the respective activities. By calculating the difference between the maximum and minimum

angles, the range of motion for each axis of the hip joint was obtained. Statistical methods were then employed to assess the variability of the range of motion among the defined population. Mean and standard deviation calculations were performed to quantify the amount of variability in the calculated range of motion for each activity. The mean value represented the average range of motion, while the standard deviation provided insights into the dispersion or spread of the data around the mean. A lower standard deviation indicated higher accuracy and repeatability of the measurements, suggesting a more consistent range of motion across the population. By adding and subtracting the calculated standard deviation from the mean of the data, the upper and lower limits for the range of motion could be determined. These limits represented the range within which the majority of the data points fell, indicating the expected variability in the range of motion for each activity among the volunteers. It was able to quantify the variability in hip joint motion across different activities and assess the consistency of the measurements within the defined subject by employing these statistical measures,. This information was valuable for understanding the characteristics and potential limitations of hip joint motion in various functional tasks and could contribute to the development of targeted interventions or rehabilitation strategies. Although there were variations in the range and values among individual volunteers, a consistent pattern in the curves was observed for each activity. This suggests that while the specific values may differ, the overall trends and movement patterns of the hip joint during the activities were similar among the participants. These findings provide valuable insights into the range of motion variability of the hip joint during different activities and contribute to understanding the collective behavior of the hip joint within the defined population. The observed patterns and variations can aid in developing targeted interventions, designing customized rehabilitation programs, or optimizing biomechanical models for further analysis. The results obtained from the analysis of each set of activity are visually presented through plots, accompanied by corresponding tables. These plots provide a clear visualization of the range of motion data for the hip joint, while the tables offer concise numerical values for reference.

In Figure 20, the plotted graphs depict the range of motion for each activity. The legend of the graphs includes important information, such as the mean value, upper boundary, and lower boundary of the range of motion. This legend serves as a guide for interpreting the graphs and understanding the variability of the data.

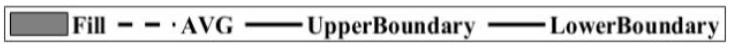

Figure 20. Legends of Result Plots

The figures presented illustrate the angular range of motion for each set of activity, represented as a percentage of the complete activity cycle. Each activity is assigned a 100% range to represent a full cycle. However, since the duration of performing each activity may vary among volunteers, a normalization process was employed to ensure consistency and eliminate subjectivity in the analysis.

The normalization process involved converting the time values into cycle percentages. This was achieved by interpolating the selected sample time as a reference point and mapping it to the corresponding cycle percentage. By doing so, the time dependency was removed, allowing for a standardized comparison of range of motion variability across different activities and subjects.

3.1.1. Stair Climbing

This study focused on investigating the kinematic and kinetic characteristics of the lower extremity during the initiation and end stages of stair climbing in a controlled laboratory environment. It utilized a motion capture system to capture detailed movement data. However, it is important to acknowledge that the study has certain limitations that should be taken into consideration when interpreting the results.

One limitation is the participant sample, which consisted only of healthy young adults. This means that the findings may not be directly applicable to other populations, such as the elderly or individuals with specific health conditions like osteoarthritis or other diseases. Previous research has shown that there can be significant differences in kinematic parameters during stair climbing between different age groups or individuals with specific health conditions. Therefore, caution should be exercised when generalizing the findings of this study to other populations.

It is worth noting that a previous study comparing stair climbing analysis in elderly individuals and healthy young subjects reported significant differences in kinematic parameters. This highlights the importance of considering age-related factors and specific health conditions when studying stair climbing or other functional tasks.

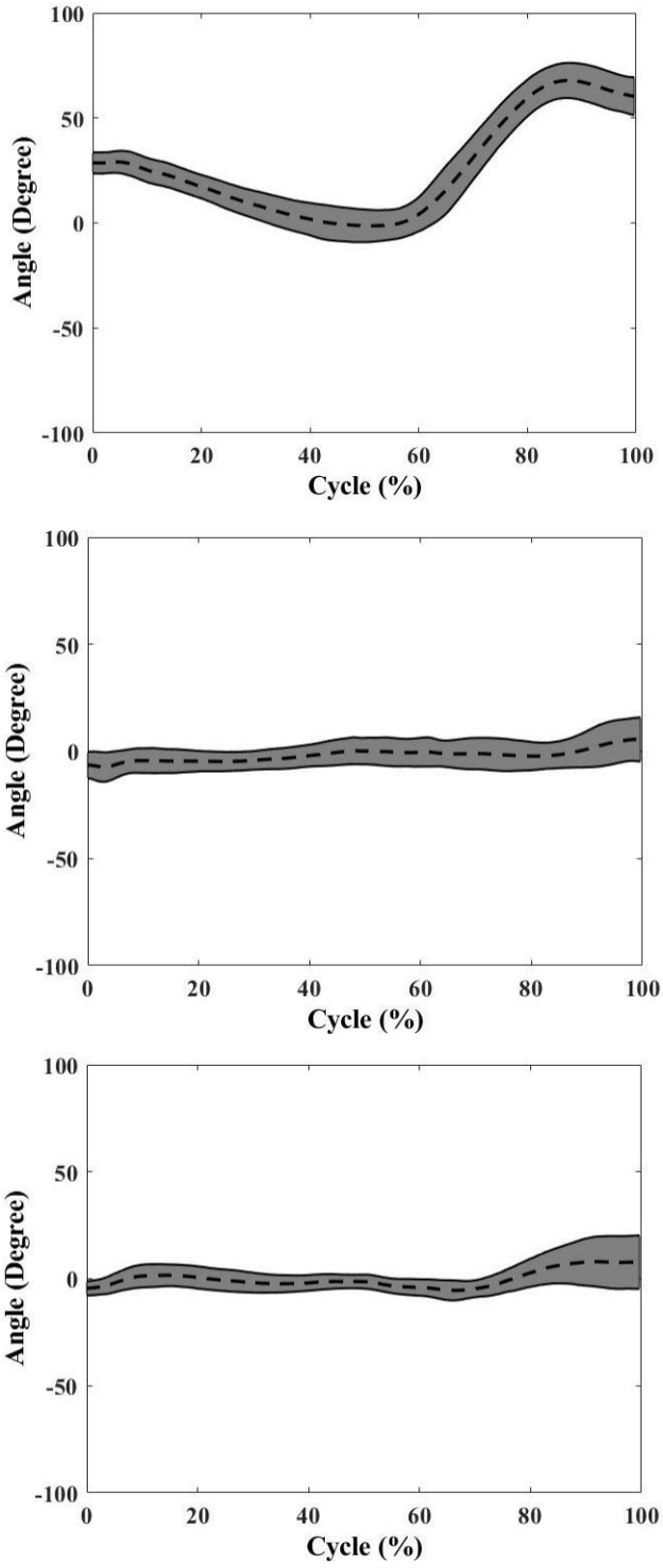

Figure 21. Angle Plot of The Hip Joint for Stair Climbing

As seen in Table 7, the hip joint has 68.97° of flexion – extension range of motion with a standard deviation of 23.42°. The hip abduction – adduction has an 17.45° range of motion. The hip internal – external rotation has a 16.40 ° range of motion. The graphical representation of a normal subject's hip joint movement reveals distinct patterns during the gait cycle. Specifically, during the ascent phase, two peaks of hip flexion can be observed.

During the ascent phase, the hip joint initially flexes during the stance phase, indicating the bending of the hip as the leg moves forward. After reaching its maximum flexion, the hip joint gradually increases its flexion until it reaches a maximum value at approximately from 60% of the gait cycle.

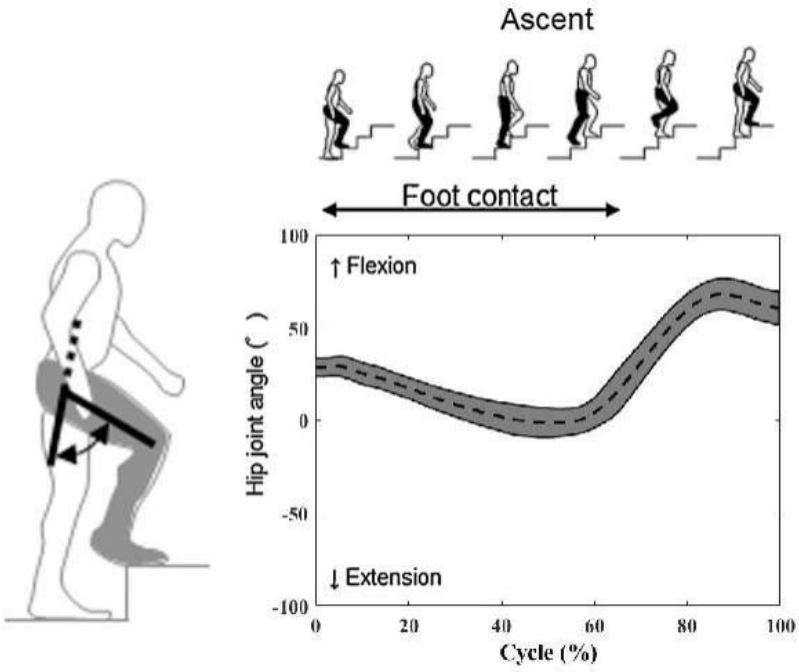

Figure 22. Hip Flexion During Ascent

Table 7. Max., min., and RoM Values of Hip Stair Climbing

STAIR CLIMBING			
	Max.	**Min.**	**Range of Motion**
Hip F-E	74.92	5.95	68.97
Hip ABD-ADD	15.22	-2.23	17.45
Hip I-E ROT	15.20	-1.20	16.40

The range of hip flexion, which represents the difference between the maximum and minimum flexion values, is approximately 68 degrees. This measurement provides an indication of the extent of hip movement throughout the gait cycle for the specific subject analyzed.

These findings contribute to our understanding of the kinematics of the hip joint during gait and provide valuable insights into the normal movement patterns observed in healthy individuals. The graphical representation and quantification of hip flexion dynamics offer important information for assessing and comparing hip joint function in clinical conditions.

External-rotation and abduction movements must be exposed in order to keep the center of gravity in the midline during hip flexion and extension movements. That is, no movement occurs in one dimension.

Hip external-rotation and abduction correlate because they originate from the angle of anteversion of the hip joint. Indicates the accuracy of the movement. It shows that due to the anatomical structure of the femur bone, hip abduction cannot be exposed without external rotation. When the graphics are examined, the external rotation and abduction that occur on the body biomechanics keep the energy to a minimum by expanding the support surface.

The increase in external-rotation movement during stair climbing showed a parallel increase with the increase in height from the ground.

As seen in Figure 23, The external joint moments recorded in our study showed that the hip extensor muscles should be activated to counter the flexion moment of the hip during stair climbing. When paired with low intra-subject variability of frontal plane hip moments, this means tight motor control may be a strategy to improve stability. There is a situation where the moments of the hip abductors are important for climbing stairs safely. Hip abductor moments are related to frontal plane balance and are required during weight acceptance and controlled lowering of the pelvis.

The anterior/posterior (A/P) moment arms are typically smaller compared to straight walking during stair conditions, This is primarily because foot placement during stair climbing is constrained by the depth of the step, which limits the extent to which the foot can be positioned anteriorly or posteriorly. In contrast, during straight walking, foot placement is not restricted, allowing for a wider range of A/P foot placement.

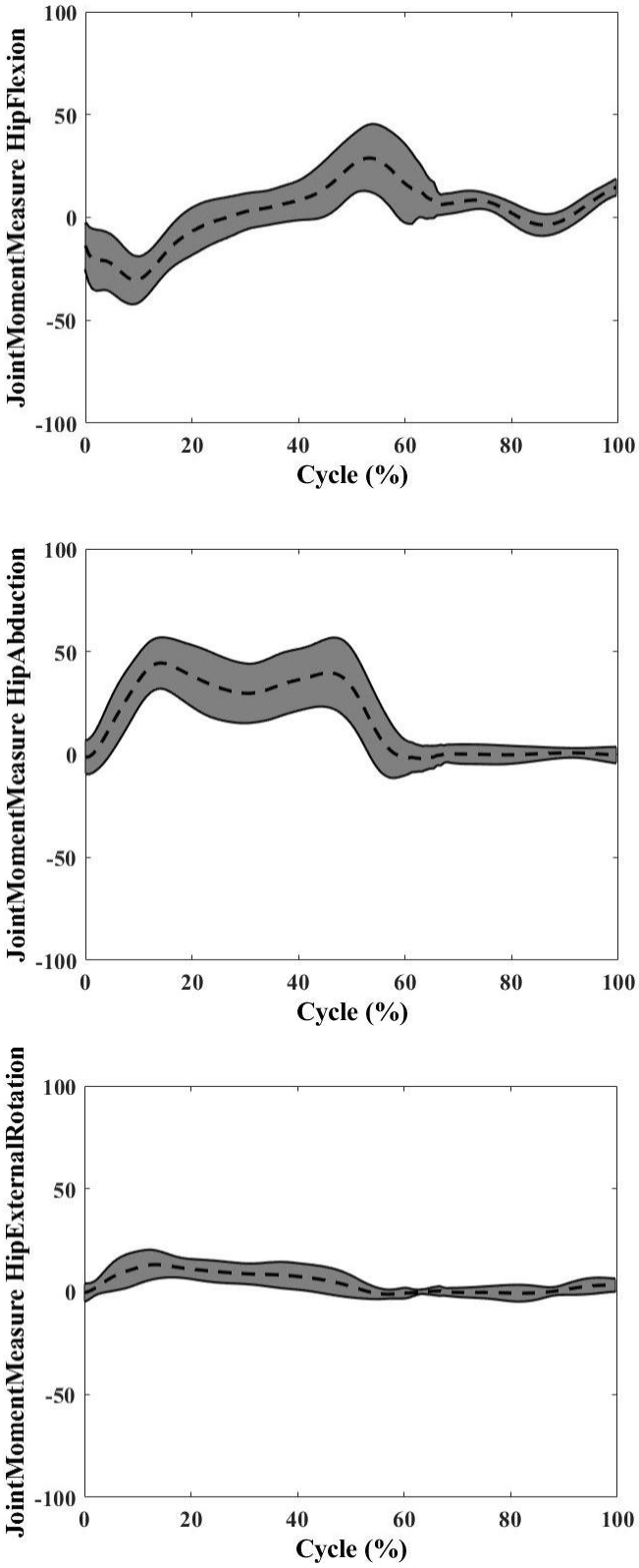

Figure 23. Moment of Stair Climbing

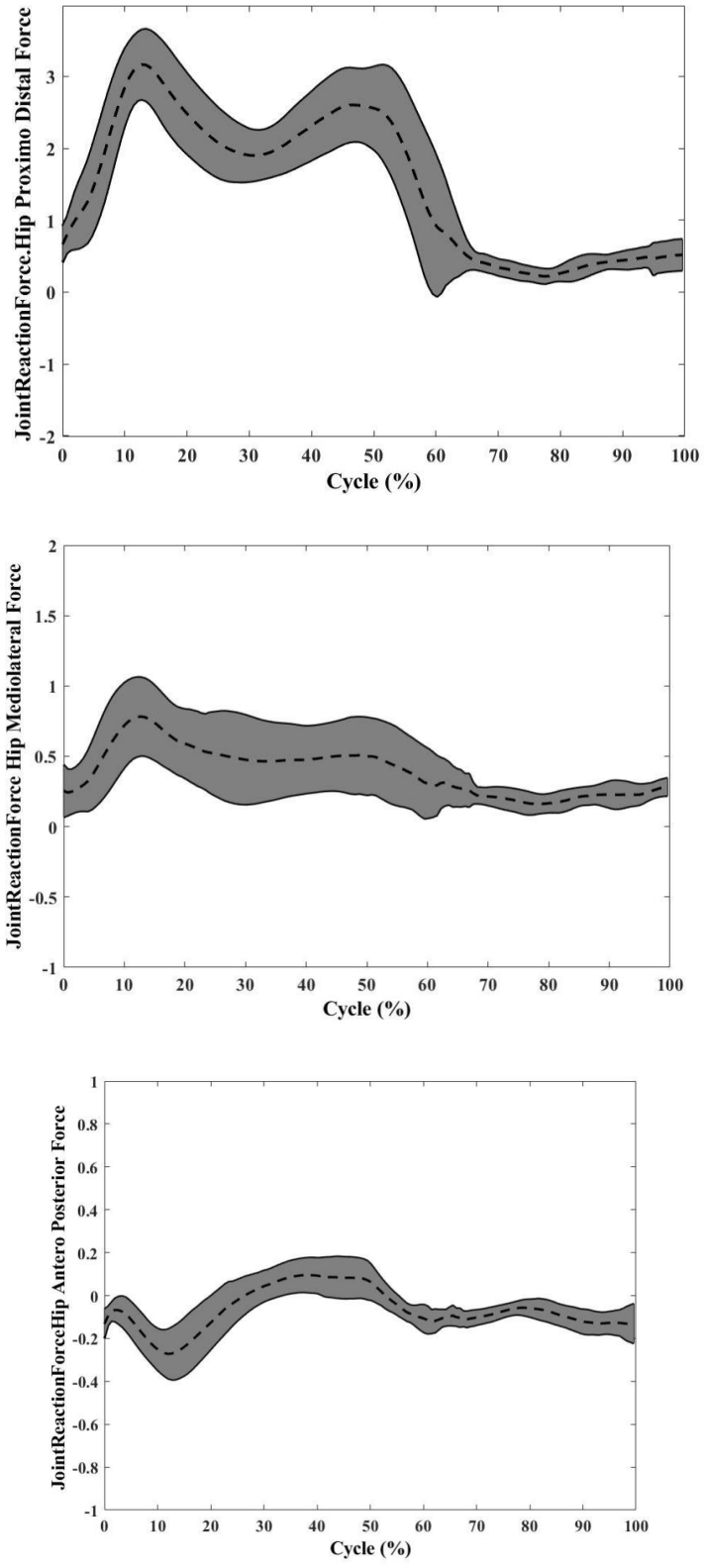

Figure 24. GRF of Stair Climbing

As seen in Figure 24 , In terms of medial/lateral (M/L) moment arms, they tend to be larger during stair walking compared to straight walking. This is likely due to the need for greater balance control and lateral stability during stair climbing, which requires more active control of the foot position to maintain stability on the smaller support surface of the step. Furthermore, the anterior/posterior ground reaction forces (GRFs) during stair walking are generally smaller compared to straight walking. This results in a smaller external moment around the joints during specific phases of the gait cycle, typically ranging from 0% to 10% and 50% to 60%. The reduced A/P GRFs during stair walking can be attributed to the constraints imposed by the step depth and the need for controlled foot placement on the step surface.

3.1.2. Cycling

As seen in Table 8, the hip joint has 25.25° of flexion – extension range of motion .The hip abduction – adduction has an 3.36° range of motion. The hip internal – external rotation has a 16.40 ° range of motion.

Table 8. Max., min., and RoM Values of Hip Cycling

CYCLING			
	Max.	**Min.**	**Range of Motion**
Hip F-E	81.74	56.49	25.25
Hip ABD-ADD	-3.36	-6.72	3.36
Hip I-E ROT	1.09	-3.55	4.64

The cycling shows extension in 50 percent of the rotation movement and hip flexes in the second 50 percent. In the moment graph, on the other hand, the reason for the zeroing of the moment at the end of the extension movement is that it starts a new movement.

During the first 180 degrees of crank rotation, There was a change in moments of force in each of the three joints studied. This can be attributed to the increased demand for propulsion during this stage of the cycling motion. The larger muscle groups of the thigh likely played a more active role in generating force and pushing against the pedals.

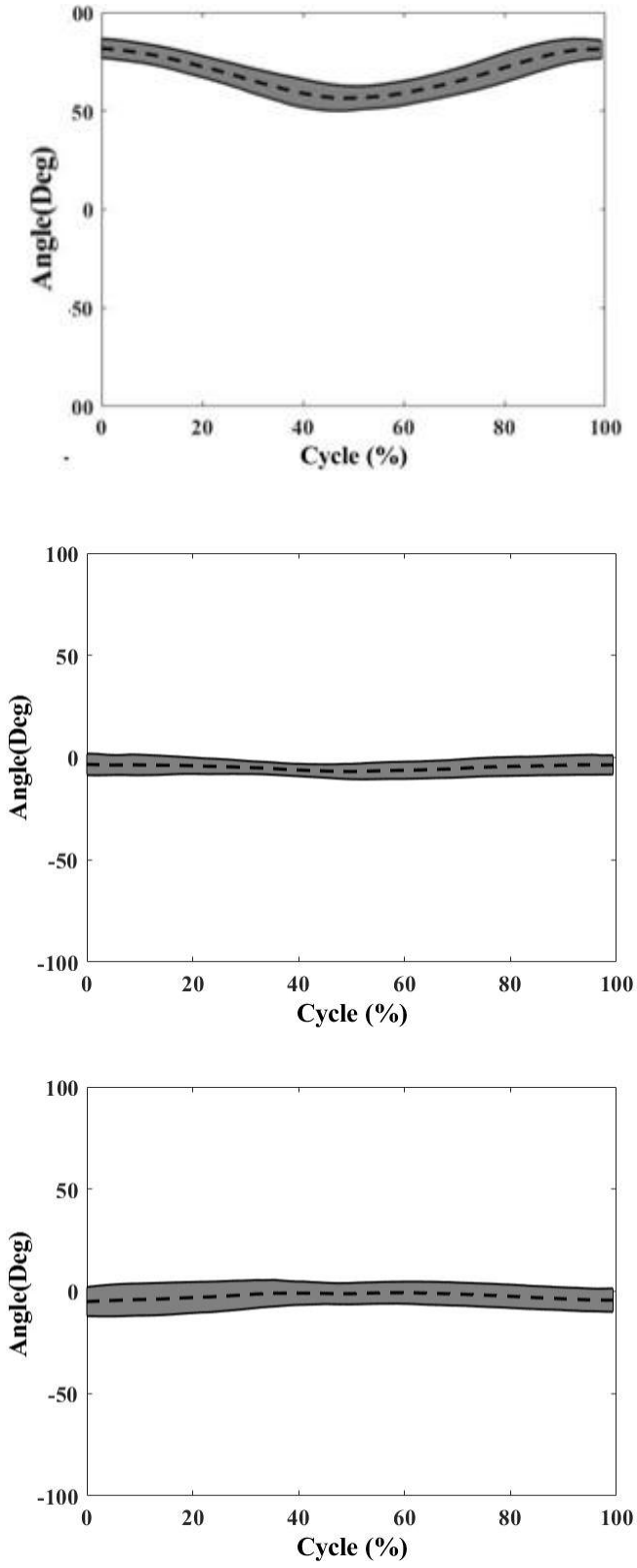

Figure 25. Angle Plot of The Hip Joint for Cycling

The min. moment of abduction is the moment released for positioning the hip. External Rotation and Abduction are close to zero since the movement during sitting is in a single plane.

At the same time, the smaller plantar flexor muscles of the lower leg may have experienced some degree of fatigue, resulting in a relatively reduced contribution to force production. This shift in muscle involvement could explain the observed increase in moments of force at the hip and knee joints, as these larger muscle groups took on a more dominant role.

To compensate for the increased force demands during the pushing phase, the ankle plantar flexor moment also increased. This adjustment in the ankle joint helped maintain a constant power output applied by the subject. By increasing the plantar flexor moment, the subject was able to sustain the required force production and continue generating power efficiently throughout the crank rotation. These findings suggest that the neuromuscular system adapts to the changing demands of the cycling motion, with different muscle groups taking on varying roles at different stages of the pedal stroke. The observed increase in moments of force at the hip and knee joints, along with the compensatory increase in the ankle plantar flexor moment, reflects the complex interplay between muscle activation patterns and force production during cycling.

The finding that daily life activities, including stair climbing and cycling, have a significant impact on the hip joint in the sagittal plane is consistent with the literature survey. The sagittal plane is the primary plane of movement for activities involving lower limb function, and it plays a crucial role in generating power and propelling the body forward during locomotion.

Stair Climbing of the hip joint are in a similar trend with Anastasia Protopapadaki. (2007), P. Costigan .(2002) and Dr. Sadiq Jafer Abbass(2012) in sagittal plane. The coronal and transverse plane results similarity might be affected by the posture or performing style of the volunteer.

Moment and GRF value match all plane with Anne K. Silverman (2019). When the released moment and GRF values were compared, similar results were observed for the purposes of the study.

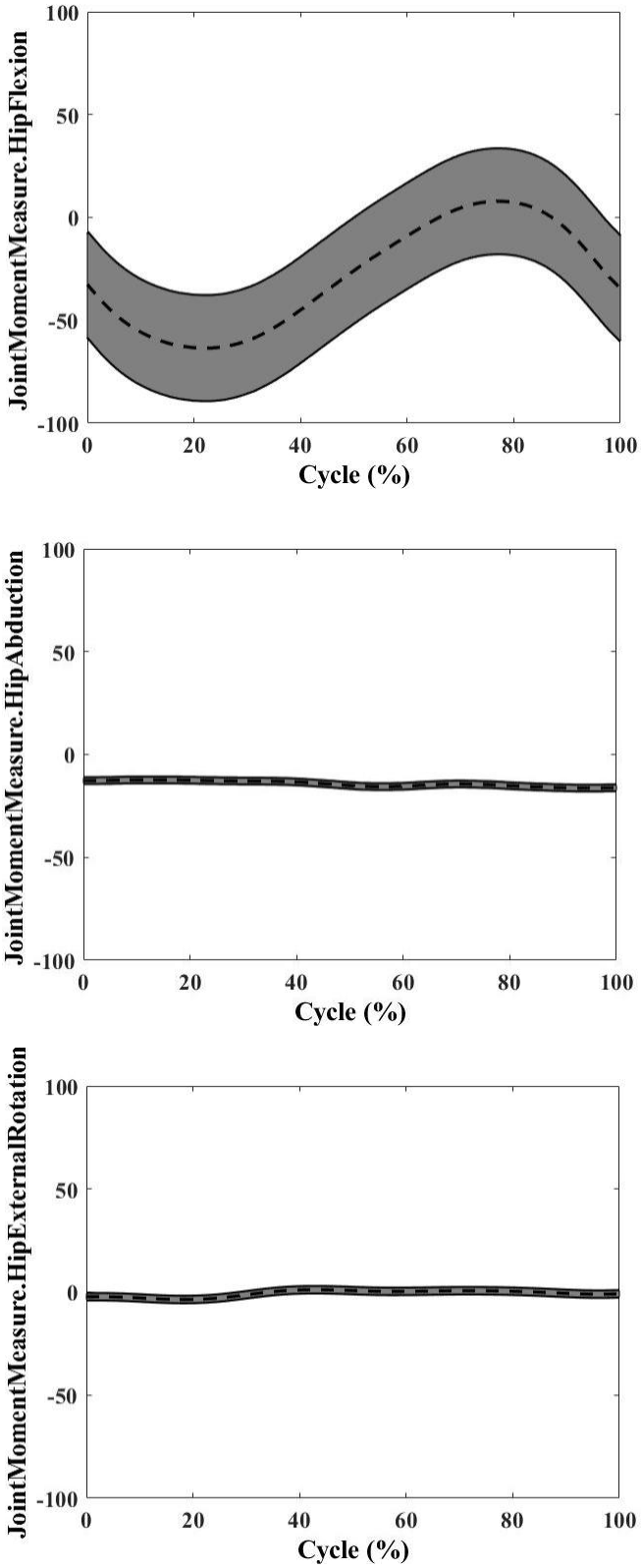

Figure 26. Moment of Cycling

Cycling of the hip joint are in a similar trend with David J Sanderson(202), Rodrigo R Bini(2010). We observe that we obtain similar results when the moments are compared in the sagittal plane.

The hip joint is a key contributor to sagittal plane movements, such as hip flexion and extension. Stair climbing and cycling require repetitive hip flexion and extension motions, making the hip joint particularly involved in these activities. The hip joint needs to exhibit a wide range of motion and generate sufficient muscle strength to perform these movements effectively.

The similarity in results between your study and the literature survey further supports the notion that daily life activities have a consistent impact on the hip joint in the sagittal plane. When different studies investigating similar activities consistently report similar findings, it enhances the understanding and knowledge of the biomechanical demands placed on the hip joint during these activities.

These findings have important implications for various fields, including clinical practice, rehabilitation, and sports performance. Understanding how daily life activities affect the hip joint in the sagittal plane can help clinicians and therapists assess and rehabilitate individuals with hip joint disorders or injuries. It can also guide the development of exercise programs and interventions aimed at improving hip joint function and preventing injuries.

Furthermore, the consistency in results emphasizes the need for individuals engaging in activities such as stair climbing and cycling to maintain hip joint health and optimize their biomechanics. Proper technique, adequate muscle strength, and appropriate training can contribute to better performance, reduced risk of injury, and overall joint health.

Overall, the convergence of findings between your study and the literature survey highlights the importance of the hip joint in sagittal plane movements during daily life activities and reinforces the existing knowledge in this field.

CHAPTER 4

CONCLUSION

In this thesis study, the focus was on investigating the kinematics of the hip joint during daily life activities, specifically stair climbing and cycling. These activities were chosen due to their repetitive nature and significant impact on the hip joint among the Turkish population.

To collect the necessary data, a gold standard motion capture system called Qualisys was utilized. Prior to data collection, a calibration process was conducted to ensure accurate measurements. Line-of-sight issues were also addressed by checking the camera setup. The workspace was prepared, and the volunteers underwent anthropometric measurements to minimize marker misplacement. Reflective markers were then placed on specific anatomical locations of each volunteer's body.

Once the volunteers were prepared, a static calibration pose was captured. This static pose served as a crucial reference for segment definition during the analysis phase. Additional markers were removed, and the activities were performed by the volunteers, mimicking their natural movements in daily life. Comfort and naturalness of movement were emphasized to ensure the collection of authentic data representing the target population.

Each activity was recorded for a defined cycle, and the collected data was processed in Qualisys Track Manager (QTM) for marker labeling. The labeled activity files were then exported as C3D files, containing all the necessary information for inverse kinematics calculations. These C3D files were subsequently used in software such as OpenSim and Anybody to build full body models based on the static pose and marker set definitions.

A pipeline was developed to perform inverse kinematic and inverse dynamic analyses on the collected data. Statistical methods were applied to examine the range of motion variability across the volunteers. Mean and standard deviation calculations were performed, enabling the determination of upper and lower boundaries for the range of motion of the hip joint during each activity. MATLAB was used to visualize and plot the results, providing valuable insights into the variability of hip joint movement.

By analyzing data from multiple individuals, this study aimed to provide insights that could contribute to predicting movement recovery and progression in patients. The findings could potentially be utilized in developing personalized therapy protocols in rehabilitation, allowing for individualized progress monitoring. Furthermore, the data collected from this study could inform the design of optimal parameters for exercise devices and personalized implants, if necessary.

Overall, this thesis study successfully investigated hip joint kinematics during daily life activities, highlighting the importance of accurate data collection, rigorous analysis, and statistical evaluation for obtaining meaningful insights into human movement patterns.

REFERENCES

[1] S. Mihcin, “Simultaneous validation of wearable motion capture system for lower body applications: over single plane range of motion (ROM) and gait activities.”, Biomed. Tech. (Berl), c. 67, sy 3, ss. 185-199, Haz. 2022, doi: 10.1515/bmt-2021-0429.

[2] I. Muller, R. de Brito, C. Pereira, ve V. Brusamarello, “Load cells in force sensing analysis -- theory and a novel application”, IEEE Instrum. Meas. Mag., c. 13, sy 1, ss. 15-19, Şub. 2010, doi: 10.1109/MIM.2010.5399212.

[3] M. Damsgaard, J. Rasmussen, S. T. Christensen, E. Surma, ve M. de Zee, “Analysis of musculoskeletal systems in the AnyBody Modeling System”, Simul. Model. Pract. Theory, c. 14, sy 8, ss. 1100-1111, Kas. 2006, doi: 10.1016/j.simpat.2006.09.001.

[4] S. L. Delp vd., “OpenSim: Open-Source Software to Create and Analyze Dynamic Simulations of Movement”, IEEE Trans. Biomed. Eng., c. 54, sy 11, ss. 1940-1950, Kas. 2007, doi: 10.1109/TBME.2007.901024.

[5] D. Giavarina, “Understanding Bland Altman analysis”, Biochem. Medica, c. 25, sy 2, ss. 141-151, 2015, doi: 10.11613/BM.2015.015.

[6] K. J. van Stralen, F. W. Dekker, C. Zoccali, ve K. J. Jager, “Measuring Agreement, More Complicated Than It Seems”, Nephron Clin. Pract., c. 120, sy 3, ss. c162-c167, Haz. 2012, doi: 10.1159/000337798.

[7] N. A. Turpin ve B. Watier, “Cycling Biomechanics and Its Relationship to Performance”, Appl. Sci., c. 10, sy 12, s. 4112, Haz. 2020, doi: 10.3390/app10124112.

[8] Pottinger, M.V. (2018). Inverse Dynamic Analysis of ACL Reconstructed Knee Joint Biomechanics During Gait and Cycling Using OpenSim, doi:10.15368/THESES.2019.24

[9] Yum, H., Kim, H., Lee, T. et al. Cycling kinematics in healthy adults for musculoskeletal rehabilitation guidance. BMC Musculoskelet Disord **22**, 1044 (2021). https://doi.org/10.1186/s12891-021-04905-2

[10] Tang, Yunqi, Donghai Wang, Yong Wang, Keyi Yin, Cui Zhang, Limin Zou, and Yu Liu. 2020. "Do Surface Slope and Posture Influence Lower Extremity Joint Kinetics during Cycling?" International Journal of Environmental Research and Public Health 17, no. 8: 2846. https://doi.org/10.3390/ijerph17082846

[11] Abbass, S.J. (2012). Biomechanical Analysis of Human Stair Climbing (Ascending and Descending).

[12] Pickle, N. T., Wilken, J. M., Aldridge, J. M., Neptune, R. R., & Silverman, A. K. (2014). Whole-body angular momentum during stair walking using passive and powered lower-limb prostheses. Journal of biomechanics, 47(13), 3380–3389. https://doi.org/10.1016/j.jbiomech.2014.08.001

[13] Bertec (2016) 'Force Plate FP4060-08', pp. 7–8.

[14] BEST Performance Group, "Optical Motion Capture.", (2015), Available online (2022)at: www.bestperformancegroup.com/?page_id=31

[15] C3d.org, "Tthe 3D standard", (2022). Available online (2022) at: www.c3d.org.

[16] Gregor, R. J., & Wheeler, J. B. (1994). Biomechanical factors associated with shoe/pedal interfaces: Implications for injury. Sports Medicine, 17, 117-131.

[17] Protopapadaki, A., Drechsler, W.I., Cramp, M., Coutts, F.J., & Scott, O.M. (2007). Hip, knee, ankle kinematics and kinetics during stair ascent and descent in healthy young individuals. Clinical biomechanics, 22 2, 203-10 doi:10.1016/J.CLINBIOMECH.2006.09.010

[18] Sanderson, D. J., & Black, A. (2003). The effect of prolonged cycling on pedal forces. Journal of sports sciences, 21(3), 191–199. https://doi.org/10.1080/0264041031000071010

[19] Human-Motion Capture, "Electromagnetic Measurement Systems." Accuracy of Human Motion Capture Systems for Sport Applications, (2018). Available online (2022) at: human-motioncapture.com/measurement-systems/electromagnetic-measurement-systems.

[20] Mihcin, Senay, et al. (2020), "Wearable Motion Capture System Evaluation for Biomechanical Studies for Hip Joints." Journal of Biomechanical Engineering, Crossref, doi:10.1115/1.4049199.

[21] Qualisys, "Miqus.", (2014) www.qualisys.com/cameras/miqus. Available at: https://www.qualisys.com/cameras/miqus/#!#tech-specs (Accessed: 27 February 2021).